forests

MDPI

Article

MultiProduct Optimization of *Cedrelinga cateniformis* (Ducke) Ducke in Different Plantation Systems in the Peruvian Amazon

Juan Rodrigo Baselly-Villanueva [1,*], Andrés Fernández-Sandoval [1], Evelin Judith Salazar-Hinostroza [2], Gloria Patricia Cárdenas-Rengifo [3], Ronald Puerta [4], Tony Steven Chuquizuta Trigoso [5,*], Yennifer Lisbeth Rufasto-Peralta [5], Geomar Vallejos-Torres [6], Gianmarco Goycochea Casas [7], Carlos Alberto Araújo Junior [8], Gerónimo Quiñónez-Barraza [9], Pedro Álvarez-Álvarez [10] and Helio Garcia Leite [7]

1 Estación Experimental Agraria San Roque, Instituto Nacional de Innovación Agraria (INIA), Calle San Roque 209, Loreto 16430, Peru; afernandez@inia.gob.pe
2 Dirección de Desarrollo Tecnológico Agrario, Instituto Nacional de Innovación Agraria (INIA), Av. La Molina 1981, Lima 15024, Peru; esalazar@inia.gob.pe
3 Estación Experimental Agraria Pucallpa, Instituto Nacional de Innovación Agraria (INIA), Carretera Federico Basadre Km 4200, Pucallpa 25004, Peru; gcardenas@inia.gob.pe
4 Universidad Nacional Agraria de la Selva, Tingo Maria, Huánuco 100601, Peru; ronald.puerta@unas.edu.pe
5 Universidad Nacional Autónoma de Chota, Jr. José Osores Nro. 418, Chota 06121, Peru; rufastoyenniferlisbeth@gmail.com
6 Universidad Nacional de San Martín, Jr. Maynas No 177, Tarapoto 22200, Peru; gvallejos@unsm.edu.pe
7 Department of Forest Engineering, Federal University of Viçosa, Viçosa 36570-900, MG, Brazil; gianmarco.casas@ufv.br (G.G.C.); hgleite@ufv.br (H.G.L.)
8 Laboratório de Pesquisa Operacional e Modelagem Florestal, Universidad Federal de Minas Gerais, Belo Horizonte 31270-901, MG, Brazil; carlosaraujo@ica.ufmg.br
9 Campo Experimental Valle del Guadiana, Instituto Nacional de Investigaciones Forestales, Agrícolas y Pecuarias (INIFAP), Carretera Durango—Mezquital km 4.5, Durango 34170, Durango, Mexico; quinonez.geronimo@inifap.gob.mx
10 Department of Organisms and Systems Biology, Polytechnic School of Mieres, University of Oviedo, E-33600 Mieres, Asturias, Spain; alvarezpedro@uniovi.es
* Correspondence: jrbasellyv@gmail.com (J.R.B.-V.); tchuquizuta@unach.edu.pe (T.S.C.T.)

check for updates

Academic Editor: Phillip G. Comeau

Received: 7 December 2024
Revised: 4 January 2025
Accepted: 10 January 2025
Published: 16 January 2025

Citation: Baselly-Villanueva, J.R.; Fernández-Sandoval, A.; Salazar-Hinostroza, E.J.; Cárdenas-Rengifo, G.P.; Puerta, R.; Trigoso, T.S.C.; Rufasto-Peralta, Y.L.; Vallejos-Torres, G.; Casas, G.G.; Araújo Junior, C.A.; et al. MultiProduct Optimization of *Cedrelinga cateniformis* (Ducke) Ducke in Different Plantation Systems in the Peruvian Amazon. *Forests* **2025**, *16*, 164. https://doi.org/10.3390/f16010164

Copyright: © 2025 by the authors. Licensee MDPI, Basel, Switzerland. This article is an open access article distributed under the terms and conditions of the Creative Commons Attribution (CC BY) license (https://creativecommons.org/licenses/by/4.0/).

Abstract: This study addressed multi-product optimization in *Cedrelinga cateniformis* plantations in the Peruvian Amazon, aiming to maximize volumetric yields of logs and sawn lumber. Data from seven plantations of different ages and types, established on degraded land, were analyzed by using ten stem profile models to predict taper and optimize wood use. In addition, the structure of each plantation was evaluated using diameter distributions and height–diameter ratios; log and sawn timber production was optimized using SigmaE 2.0 software. The Garay model proved most effective, providing high predictive accuracy (adjusted R^2 values up to 0.963) and biological realism. Marked differences in volumetric yield were observed between plantations: older and more widely spaced plantations produced higher timber volumes. Logs of optimal length (1.83–3.05 m) and larger dimension wood (e.g., 25.40 × 5.08 cm) were identified as key contributors to maximizing volumetric yields. The highest yields were observed in mature plantations, in which the total log volume reached 508.1 m^3ha^{-1} and the sawn lumber volume 333.6 m^3ha^{-1}. The findings demonstrate the power of data-driven decision-making in the timber industry. By combining precise modeling and optimization techniques, we developed a framework that enables sawmill operators to maximize log and lumber yields. The insights gained from this research can be used to improve operational efficiency and reduce waste, ultimately leading to increased profitability. These practices promote support for smallholders and the forestry industry while contributing to the long-term development of the Peruvian Amazon.

Keywords: agroforestry; dynamic programming; logs; production planning; sawn lumber; taper; wood industry

1. Introduction

Plantation forests occupy a total area of about 131 million hectares worldwide, representing 3% of the global forest area and 45% of all planted forests. South America has the highest proportion of plantation forests, accounting for 99% of the planted forest area and 2% of the total forest area. Globally, 44% of plantation forests are dominated by introduced species, with significant regional variations [1,2]. For instance, plantation forests in North and Central America mainly consist of native species, while those in South America are almost exclusively composed of introduced species [3].

The rapid expansion of tree plantations, particularly in Asia and Latin America, has been a defining trend in recent decades. Annual growth rates of 2% [4,5] have led to significant increases in forested areas, primarily in countries like Vietnam, China, Chile and Brazil. These plantations often rely on exotic species, a practice that has drawn considerable attention [6,7]. The establishment of plantations using native species has gained traction globally [8,9]. However, initiatives are often limited by a lack of knowledge about the most suitable silvicultural techniques for native species [10]. The concern regarding the establishment of plantations is driven by the high demand for forest products and the decline in natural forests [11]. These concerns have also driven the need for sustainable forest management practices, including the establishment of plantations of native species [12].

The planted forest area in Peru is currently 117,579.34 hectares [13]. In the mountains, eucalyptus (*Eucalyptus* spp.) and pine (*Pinus* spp.) are the dominant species, together with native species such as quinual (*Polylepis* spp.), which is used for wood and firewood. On the coast, carob (*Prosopis pallida*) and tara (*Caesalpinia spinosa*) are important for wood and beekeeping [14]. In the jungle, the planted area is around 46,295.15 hectares (39.2%), distributed in the regions of Loreto (12.7%), San Martín (9.4%), Amazonas (8.7%), Ucayali (7.4%) and Madre de Dios (1%) [13]. Amazonian plantations are mainly established with native species such as *Cedrelinga cateniformis* (Ducke) Ducke, known as "Tornillo" [14].

Cedrelinga cateniformis is one of the main timber species in Peru. The timber is mainly obtained from natural forests, and market volumes of 115,227.96 m^3 and 69,574.17 m^3 of round and sawn wood were reached in 2023, respectively [15,16]. Since 1970, several tropical forestry projects have been implemented, and *C. cateniformis* plantations have been established [17]. The wood, which was of a medium density (0.45 g cm^{-3}), with good workability and rapid growth, is widely used in carpentry, vehicle bodies and furniture-making. The species presents good growth rates in plantations, being a valuable resource for the timber industry [18–20]. In addition, the species is also of interest to the forestry industry for the quality of its wood and its good adaptability in agroforestry systems, which is of potential value for the sustainable development of the Amazon region [21,22].

A bioeconomic model developed for *C. cateniformis* management has determined that the optimal harvest cycle to maximize economic benefits while ensuring the sustainability of the resource is 25 years [23]. The species has been the subject of various growth modeling studies in plantations in the Amazon, highlighting its economic and ecological importance [18,24,25]. Despite the prevalence of these plantations, a sustainable management strategy for remains underdeveloped.

By analyzing tree stem profiles, we can optimize harvesting and increase the economic value of each tree. This involves accurately estimating wood volume and identifying the best use for different stem sections. Forest measurement has primarily focused on describ-

ing and quantifying the irregular shapes of tree stems, as they often deviate from the ideal cylindrical form [26]. Stem profile models are mathematical representations that describe how the diameter of a tree stem tapers from its base to its crown. These models are based on various mathematical functions, such as simplified, polynomial, sigmoidal, trigonometric and segmented functions [27,28], which can be fitted using different regression techniques [29,30]. Stem profile models have been successfully applied to predict diameters at different heights and to estimate volumes within specific sections of the stem [28,31]. Although profile studies in Peru have mainly been based on shape factors [32], the use of stem profile models is less common.

Various products can be obtained from a tree for different commercial purposes, such as sawn timber, veneer, particleboard and energy. Determining the optimal quantity of products for each industry is a complex task, depending on many factors or constraints, such as log dimensions [33]. Different algorithms and programs are used for the optimization of forest products, such as the dynamic programming method, Bartho, M3to and M3sNO [34,35]. The complexity of the process depends on the degree of constraints considered and the type of objective that defines the planning [36]. Key input variables for forest product optimization typically include the following: (i) diameter distribution, (ii) product characteristics, and (iii) stem profile models [37]. Optimization solutions can be derived using linear programming, mixed-integer programming or heuristic techniques [38,39]. Effective product optimization helps maximize the value of forests and improve their productivity [40,41].

Despite the importance of *C. cateniformis* as a key timber species in the Peruvian Amazon, there are some important knowledge gaps regarding forest management and optimization potential for multi-product systems. While some studies on form factors (0.65) have been conducted in Peru [42], the use of stem profile models is less common. Previous studies have primarily focused on general growth and yield modeling [17,43] without adequately addressing the integration of advanced taper profile modeling and multi-product optimization techniques tailored to plantation structures. These limitations hinder the accurate prediction of wood volume and optimal utilization strategies, leading to inefficient resource use and generating a knowledge gap regarding the potential use of plantation wood. This situation has resulted in logging and processing practices being based on experience rather than sound technical guidelines. Furthermore, forest product optimization in Peru is not yet standard practice. Opportunities to maximize wood yield and improve the profitability of forest producers thus remain underutilized.

This study sought to address the need for adaptation strategies to improve the value of plantation wood while also addressing research gaps in stem profile modeling and forest product optimization. The specific objectives of this study were as follows: (i) to evaluate the diameter distribution and to fit models characterizing the diameter–height relationship; (ii) to identify the most suitable stem profile models for forest plantations; and (iii) to maximize the volumetric yield of logs and sawn wood for multi-product production. By achieving these objectives, this research could contribute to more efficient and sustainable forest management practices in the Peruvian Amazon, ultimately benefiting both the forest industry and smallholders.

2. Materials and Methods

2.1. Study Area

The present study was carried out in seven plantations established in the Peruvian Amazon. The specific location is in the district of San Juan Bautista, province of Maynas, Loreto region, with reference coordinates 3.952500° S and 73.413951° W and an elevation of 120 m (Figure 1). The area belongs to the "El Dorado" Experimental Annex of the

San Roque Agricultural Experimental Station (National Institute of Agrarian Innovation, INIA). The minimum and maximum temperatures in the area are 21 °C and 33 °C, and the annual precipitation is around 3000 mm [44]. The soils are mainly clay loam and loamy sand, and they are strongly acidic (4.5–4.77), with low to medium levels of organic matter (0.80%–1.77%) [45].

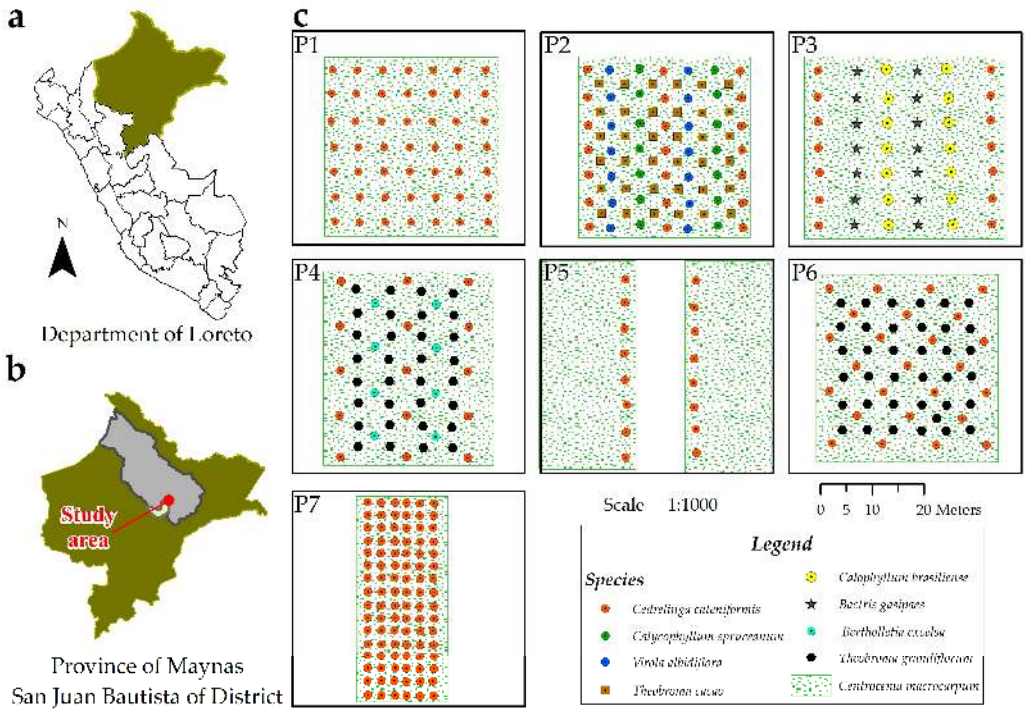

Figure 1. Location of *Cedrelinga cateniformis* plantations, Peru: (**a**) Location of the department of Loreto, (**b**) Study area, (**c**) Diagrams illustrating the different types of production systems associated with each plantation (P1 to P7).

Plantations between 10 and 35 years old were evaluated. The genetic material used for the facility is derived from botanical seeds from trees located in the natural forests surrounding the study area [46]. *C. cateniformis* is established in degraded areas of the Amazon in different types of production systems: forest massif (FM), agroforestry systems (SAF) and living fence (LF) at different spacings (Table 1). The FM corresponds to a plantation in an open area where the plants were evenly distributed; ASF are production systems where *C. cateniformis* was planted with other Amazonian forest and fruit species; and LF corresponds to an area where the species was planted at the edge of the road as a boundary (Table 1 and Figure 1).

Table 1. Descriptive detail of *Cedrelinga cateniformis* in different plantation types in the Peruvian Amazon.

Plantation	Associated Production System	Forest and Fruit Species	Area (ha)	Age (Years)	Distancing (m) (Rows/Floors)	Planting System
P-1	FM	*Cedrelinga cateniformis* + *Centrocema macrocarpum*	0.09	10	5 × 5	Square
P-2	ASF	*Cedrelinga cateniformis* + *Calycophyllum spruceanum* + *Virola albidiflora* + *Theobroma cacao* + *Centrocema macrocarpum*	1.00	10	5 × 15	Rectangle
P-3	ASF	*Cedrelinga cateniformis* + *Calophyllum brasiliense* + *Bactris gasipaes* + *Centrocema macrocarpum*	1.26	19	35 × 5	Rectangle

Table 1. *Cont.*

Plantation	Associated Production System	Forest and Fruit Species	Area (ha)	Age (Years)	Distancing (m) (Rows/Floors)	Planting System
P-4	ASF	*Cedrelinga cateniformis* + *Bertholletia excelsa* + *Theobroma grandiflorum* + *Centrocema macrocarpum*	0.54	25	12 × 8	Five-petal
P-5	LF	*Cedrelinga cateniformis* + *Centrocema macrocarpum*	0.05	29	5	Linear
P-6	ASF	*Cedrelinga cateniformis* + *Theobroma grandiflorum* + *Centrocema macrocarpum*	0.40	28	10 × 10	Five-petal
P-7	ASF	*Cedrelinga cateniformis* + *Piper nigrum* + *Centrocema macrocarpum*	0.27	35	2.7 × 2.7	Rectangle

FM: forest massif; AFS: agroforestry systems; LF: live fence.

2.2. Data Collection

All trees (100%) in the plantations were inventoried. The trees were georeferenced, and the diameter at breast height (*dbh*) and total height (*H*) were measured using diameter tape and the laser dendrometer (Criterion™ RD1000, Laser Technology, Centennial, CO, USA), respectively. Stem profile measurements were taken by section. The diameter at 0.30 and 1.3 m height was determined by measuring it with a diameter tape. The upper diameters were determined by remote measurement using a dendrometer (±1.5 cm). In trees smaller than 30 cm *dbh*, the remotely evaluated sections were measured every 2 m, and in trees larger than 30 cm *dbh*, they were measured every 3 m until reaching a stem diameter of 5 cm. At least six sections were evaluated in each tree.

2.3. Data Dendrometric Description

Dendrometric measurements of *C. cateniformis* (Table 2) were divided into training (70%) and validation (30%) data sets for the plantations (P-1 to P-7). This process ensures robust model analysis, enabling generalization beyond the training data and improving prediction accuracy and reliability for future applications. The variables include the total number of data measured (N), number of trees (n), diameter at breast height (*dbh*), tree height (*H*), diameter (*d*) at a certain height *h* along the stem and (h), which is the height from the base to the point where the diameter *d* is reached. For each variable, the table provides average, maximum, minimum and standard deviation values. In the training data, the average *dbh* ranged from 21.83 cm (P-1) to 51.15 cm (P-5), which is similar to the validation means. The maximum *dbh* value recorded was 109.60 cm (P-5), while the minimum was 7.90 cm (P-2). The height (*H*) of all mean trees ranged from 14.68 m (P-2) to 29.04 m (P-4) in the training data and from 14.94 to 28.93 m in the validation data. The standard deviations for these variables indicate variability across the dataset, particularly in diameter and height, suggesting a wide range of tree sizes within the plantations.

Comparative analysis of the d/dbh ratio and relative height (h/H) by data type (training and validation) in different production systems is shown in Figure 2. Graphs of these relationships demonstrate that there are no outliers and that the data are balanced.

2.4. Stem Profile Modeling

Ten stem profile models were evaluated for *C. cateniformis* (Table 3), considering various mathematical relationships between *h*, *H* and/or *dbh*. The statistical analysis was performed using the statistical software R Studio (v. 4.3.3) [47]. The fits were conducted using the "lm" and "nls" functions for polynomial and non-linear models, respectively. The statistical significance of the model parameters was determined using the t-Student test ($\alpha \leq 0.05$) based on the fitting data; models whose parameters did not meet this criterion were rejected.

Table 2. Dendrometric measurements of *Cedrelinga cateniformis* individuals evaluated in different types of plantations in the Peruvian Amazon.

Plantation	**P-1**		**P-2**		**P-3**		**P-4**		**P-5**		**P-6**		**P-7**	
Data	**Training**	**Validation**	**Training**	**Validation**	**Training**	**Validation**	**Training**	**Validation**	**Training**	**Validation**	**Training**	**Validation**	**Training**	**Validation**
N (trees ha^{-1})	180	77	422	184	240	101	163	62	311	141	344	150	487	205
n	30	13	68	29	35	15	28	12	41	18	45	19	61	26
Average of *dbh* (cm)	21.83	20.22	24.04	23.89	47.62	45.42	49.67	50.3	51.15	51.64	35.57	41.67	43.28	43.79
Max of *dbh* (cm)	29.0	29.8	39.6	39.1	72.3	60.8	85.6	70.3	109.6	95.4	58.4	68.3	78.50	96.90
Min of *dbh* (cm)	11.1	8.4	7.9	8.7	19.6	30.8	21.9	30.5	15.5	18	16.2	23.9	17.10	12.40
StdDev of *dbh*	4.46	4.48	7.14	7.91	13	8.14	12.42	13.49	22.26	19.6	10.85	11.39	14.97	19.35
Average of *H* (m)	15.21	14.94	14.68	15.18	27.09	27.15	29.04	27.21	25.94	25.56	19.51	20.87	27.03	28.93
Max of *H* (m)	17.8	16.9	20	20.5	35.5	32.2	36.96	31.95	33.5	31.2	24.5	26.3	40.00	42.10
Min of *H* (m)	10.2	8.9	5.2	7.8	14	19.7	19.24	22.35	13.8	15.1	13.6	13.1	13.70	13.30
StdDev of *H* (m)	1.69	2.01	2.67	2.74	4.52	3.85	3.8	2.94	5.6	3.76	2.92	3.59	5.69	7.29
Average of *d* (cm)	18.45	17.53	19.85	19.79	37.39	35.78	40.76	41.03	39.52	39.19	26.82	31.22	32.75	33.99
Max of *d* (cm)	34.4	37.2	47.8	49.1	82.5	69.1	98.6	81.9	122.2	118.8	67.5	84.3	103.90	118.90
Min of *d* (cm)	7.4	5.0	5.6	5.6	7.7	12.3	11.6	12.4	9.1	7.6	7	10.3	7.80	7.70
StdDev of *d*	6	6.22	8.3	8.91	14.79	12.65	15.63	16.92	22.38	20.84	12.96	14.93	15.52	18.80
Average of *h* (m)	3.67	3.62	3.96	4.12	6.58	6.45	7.13	6.08	7.88	7.98	5.48	5.73	8.24	8.19
Max of *h* (m)	10	10	13.5	14	21	18	26.18	21.74	24	24	16	16	24.00	24.00
Min of *h* (m)	0.3	0.3	0.3	0.3	0.3	0.3	0.5	0.5	0.3	0.3	0.3	0.3	0.30	0.30
StdDev of *h*	2.84	2.86	3.17	3.34	5.35	5.23	6.45	5.88	6.42	6.38	4.21	4.46	6.51	6.58

dbh is the diameter at breast height at 1.3 m above ground level, in cm. *d* is the diameter with bark at height *h*, in cm. *H* is the total height of the tree in m. *h* is the height from the base of the tree to the point where diameter *d* is reached in m.

The model performance was determined using validation data. The adjusted coefficient of determination (R^2_{adj}; Equation (11)), coefficient of correlation between observed values and estimated values ($r_{Y\hat{Y}}$, Equation (12)), root mean square error (RMSE; Equation (13)) and percentage (RMSE%; Equation (14)), bias (Bias; Equation (15)) and its percentage (Bias%; Equation (16)), and the Akaike Information Criterion (AIC; Equation (17)) were evaluated. The models were also graphically assessed by evaluating (i) relative residual (RE%) vs. predicted diameter (*d*) and (ii) model function vs. field-observed data; the RE% was calculated using Equation (18). The model selected to explain the species profile was based on statistical indicators and biological realism.

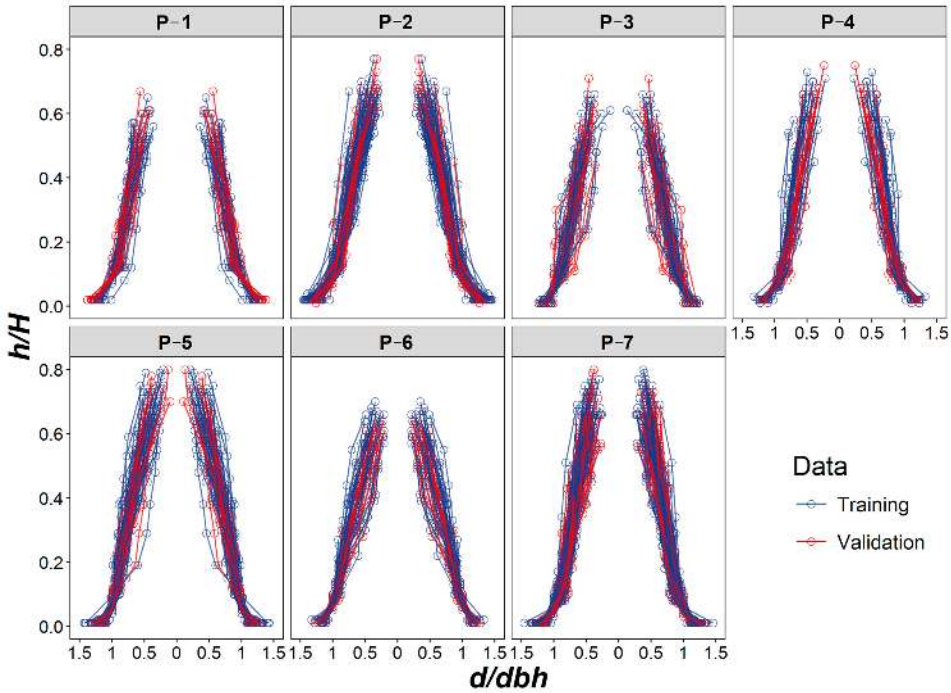

Figure 2. Relationship between diameter (*d*/*dbh*) and relative height (*h*/*H*) by data type for *Cedrelinga cateniformis*. The individual trees are represented by continuous lines.

Table 3. Stem profile models evaluated for *Cedrelinga cateniformis* trees distributed in different types of plantations in the Peruvian Amazon.

Model	Function	Author	Equation
Cielito I	$d = dbh\cdot\left[\beta_1\cdot\left(\frac{H-h}{H}\right) + \beta_2\cdot\left(\frac{H-h}{H}\right)^2 + \beta_3\cdot\left(\frac{H-h}{H}\right)^3\right]^{1/2} + \varepsilon$	[48]	(1)
Cielito II	$d = dbh\cdot\left[\beta_0 + \beta_1\cdot\left(\frac{h}{H}\right) + \beta_2\cdot\left(\frac{h}{H}\right)^2 + \beta_3\cdot\left(\frac{h}{H}\right)^3 + \beta_4\cdot\left(\frac{h}{H}\right)^4\right]^{1/2} + \varepsilon$	[48]	(2)
Clutter	$d = \beta_0\cdot dbh^{\beta_1}\cdot H^{\beta_2}\cdot(H-h)^{\beta_3} + \varepsilon$	[49]	(3)
Amidon	$d = dbh\cdot\left[\beta_1\cdot\left(\frac{H-h}{H-1.3}\right) + \beta_2\cdot\left(\frac{(H^2-h^2)\cdot(h-1.3)}{dbh\cdot H^2}\right)\right] + \varepsilon$	[50]	(4)
Kozak	$d = dbh\cdot\left[\beta_0 + \beta_1\cdot\left(\frac{h}{H}\right) + \beta_2\cdot\left(\frac{h}{H}\right)^2\right]^{1/2} + \varepsilon$	[51]	(5)
Demaerschalk	$d = 10^{\beta_0}\cdot dbh^{\beta_1}\cdot H^{2\cdot\beta_2}\cdot(H-h)^{2\cdot\beta_3} + \varepsilon$	[52]	(6)
Ormerod	$d = dbh\cdot\left(\frac{H-h}{H-1.3}\right)^{\beta_1} + \varepsilon$	[53]	(7)
Cervera	$d = dbh\cdot\left[\beta_0 + \beta_1\cdot\left(\frac{h-1.3}{H-1.3}\right) + \beta_2\cdot\left(\frac{h-1.3}{H-1.3}\right)^2 + \beta_3\cdot\left(\frac{h-1.3}{H-1.3}\right)^3 + \beta_4\cdot\left(\frac{h-1.3}{H-1.3}\right)^4\right]^{1/2} + \varepsilon$	[54]	(8)
Garay	$d = dbh\cdot\beta_0\cdot\left[1 + \beta_1\cdot\mathrm{Ln}\left(1 - \beta_2\cdot h^{\beta_3}\cdot H^{-\beta_3}\right)\right] + \varepsilon$	[55]	(9)
COFORD e IFER	$d = 2\cdot\left[\frac{\beta_1}{1-e^{\beta_2\cdot(1.3-H)}} + \left(\frac{dbh}{2} - \beta_1\right)\cdot\left(1 - \frac{1}{1-e^{\beta_3\cdot(1.3-H)}}\right) + \frac{\left(\frac{dbh}{2}-\beta_1\right)\cdot e^{1.3\cdot\beta_3}}{1-e^{\beta_3\cdot(1.3-H)}}\cdot e^{-\beta_3 h} - \frac{\beta_1 e^{-\beta_2\cdot H}}{1-e^{\beta_2\cdot(1.3-H)}}\cdot e^{\beta_2\cdot h}\right] + \varepsilon$	[56]	(10)

d is the diameter with bark at height *h*, in cm. *dbh* is the diameter at breast height at 1.3 m above ground level, in cm. *h* is the height from the base of the tree to the point where diameter *d* is reached in m. *H* is the total height of the tree in m. e is the exponential. Ln is the natural logarithm. β_0, β_1, β_2, β_3, β_4 are model parameters. ε is the random error.

$$R^2_{adj} = 1 - \frac{(n-1)\sum_{i=1}^{n}(Y_i - \hat{Y}_i)^2}{(n-p)\sum_{i=1}^{n}(Y_i - \overline{Y})^2}, \quad (11)$$

$$r_{Y\hat{Y}} = \frac{n^{-1}\left(\sum_{i=1}^{n}(\hat{Y}_i - \hat{Y}_m)(Y_i - \overline{Y})\right)}{\sqrt{\left(n^{-1}\cdot\sum_{i=1}^{n}(\hat{Y}_i - \hat{Y}_m)^2\right)\left(n^{-1}\cdot\sum_{i=1}^{n}(Y_i - \overline{Y})^2\right)}}; \hat{Y}_m = n^{-1}\sum_{i=1}^{n}\hat{Y}_i, \quad (12)$$

$$RMSE = \sqrt{\frac{\sum_{i=1}^{n}(Y_i - \hat{Y}_i)^2}{n}}, \quad (13)$$

$$RMSE\% = 100\cdot\overline{Y}_i^{-1}\sqrt{\frac{\sum_{i=1}^{n}(Y_i - \hat{Y}_i)^2}{n}}, \quad (14)$$

$$Bias = \sum_{i=1}^{n}\frac{(\hat{Y}_i - Y_i)}{n}, \quad (15)$$

$$Bias\% = 100.\overline{Y}_i^{-1}\sum_{i=1}^{n}\frac{(\hat{Y}_i - Y_i)}{n}, \quad (16)$$

$$AIC = n\cdot\log\hat{\sigma}^2 + 2\cdot K, \quad (17)$$

$$RE\% = 100\cdot\left(\frac{\hat{Y}_i - Y_i}{Y_i}\right), \quad (18)$$

where Y_i, $\hat{Y}_i$ and $\overline{Y}$ are the observed, predicted and average diameter values along the stem, respectively; n is the total number of data points used in the model fitting; log is base 10 logarithm; $K = p + 1$; p is the number of parameters to be estimated; and $\hat{\sigma}^2$ is the variance of the model error expressed as $\sum_{i=1}^{n}(Y_i - \hat{Y}_i)^2/n$.

2.5. Diameter Distribution and the Diameter-Height Relationship

The diameter distribution in each plantation was categorized in 5 cm intervals to establish diameter classes. The diameter–height relationship was assessed using five height–diameter models [57] (Table 4). These models were specifically designed to estimate the height (*H*) for the established diameter classes. The model parameters were validated using Student's *t*-test ($\alpha \leq 0.05$), and the goodness of fit was evaluated using R^2.

Table 4. Height–diameter relationship models for *Cedrelinga cateniformis* trees distributed in different types of plantations in the Peruvian Amazon.

Model Type	Function	Equation
Chapman-Richards	$H = \beta_0\cdot(1 - e(-\beta_1\cdot dbh))^{\beta_2} + \varepsilon$	(19)
Exponential	$H = \beta_0\cdot e\left(\frac{\beta_1}{dbh+\beta_2}\right) + \varepsilon$	(20)
Reciprocal	$H = \beta_0 + \beta_1\cdot\left(\frac{1}{dbh^2}\right) + \varepsilon$	(21)
Logarithmic	$\mathrm{Ln}H = \beta_0 + \beta_1\cdot\mathrm{Ln}(dbh) + \varepsilon$	(22)
Reciprocal-Log	$\mathrm{Ln}H = \beta_0 + \beta_1\cdot\left(\frac{1}{dbh}\right) + \varepsilon$	(23)

dbh is the diameter at breast height at 1.3 m above ground level, in cm. *H* is the total height of the tree in m. e denotes exponential. log denotes natural logarithm. β_0, β_1 are model parameters. ε is the random error.

2.6. Multi-Product Optimization

Multi-product optimization was carried out using SigmaE 2.0 software. This software, developed through dynamic programming, addresses the primary problem of obtaining the largest volume of harvestable stem and the highest economic yield, considering the characteristics of the forest population and the products for different industries [58]. The computational code MPDAMA (Dynamic Programming Model for the Evaluation of Multi-

Products from Individual Trees) was used [59]. The model levels and variables and the deterministic recurrence relationships are detailed below.

2.6.1. Model Levels

- First Level:

This level determines the taper profile of the tree trunk by applying equations to calculate diameter variations along its length. Based on these measurements, the trunk is sectioned into logs, and their volumes are estimated using Smalian's formula (Supplementary S1, Figure 1a).

- Second Level:

Logs are converted into products based on conversion factors obtained from industry (Supplementary S1, Figure 1b).

- Third Level:

At this stage, the logs are processed into sawn wood, defining cutting stages along the trunk. This accounts for both parallel and circular saw cuts, with parameters such as cutting thickness adjusted for each level. The optimization of product recovery is achieved using Pythagoras' theorem, and efficiency is maximized without predefining cutting structures (Supplementary S1, Figure 1c).

2.6.2. Model Variables

The model uses the following variables:

H, *Hc*, *Hb*: Total height, commercial height and remaining stump height (in meters).
dbh: Diameter at breast height measured at 1.3 m (in cm).
Kz, Kx, Ky: Intervals of states at Levels 1, 2 and 3 in the dynamic programming model.
nz.kz: Variable associated with states at Level 1 (in meters).
nx.kx, ny.ky: Variables associated with states at Levels 2 and 3 (in mm).
Nz, Nx, Ny: Total number of states at Levels 1, 2 and 3, respectively

$$\mathrm{N_z} = \frac{H_c - H_b}{\mathrm{k_z}}$$

u: Wood usage.
dmin(i), dmax(i): Minimum and maximum diameters of the *ith* log (in cm).
LZUu, LZLu: Maximum and minimum acceptable log lengths for usage *u* (in meters).
LZ[u, i]: Length of the *ith* log for usage *u* (in meters).
LZmim, LZmax: Minimum and maximum log lengths across all usages.
Piuw: Market price of the *wth* final product from the *ith* log for usage *u*.
Qiuw: Quantity of the *wth* final product from the *ith* log for usage *u*.
Cyiuw: Cost of the *wth* final product from the *ith* log for usage *u*, with components,

- Peeling cost;
- Transport cost;
- Sectioning cost;
- Processing cost (industrial).

jz.kz: State of the system, describing the current situation (number of intervals *kz* forming a log).
Vu(i): Volume of the *ith* log for usage *u* (in m^3).
FTuw: Conversion factor for usage *u* to produce final product *w*.
skz, skx, sky: Cutting thicknesses at Levels 1, 2 and 3 (in mm).
$Nx = d_{min(i)}/Kx$

- Ny;
- $y[nx]/ky$, se $y[nx] \leq y[nx - Lx[z]]$;
- $y[nx - Lx[z]]/ky$, se $y[nx] > y[nx - Lx[z]]$;
- y[nx]: Available face in state nx at Level 2;
- Lx[z]: Decision variable at Level 2 (equals product thickness w obtained between consecutive states);
- Ly[z]: Decision variable at Level 3 (corresponding to product width w obtained).

Fnz, Fnx, Gny: Optimal accumulated values at states nz, nx and ny of Levels 1, 2 and 3, respectively.
Ru(Jz.kz, dmin(i), dmax(i)): Return from converting the *ith* log of length *Jz.kz* with diameters dmax(i) and dmin(i) for usage u
V(w, nxkx, nyky, lx[z], ly[z]): Value of product w obtained at coordinates $nxkx$ and $nyky$, with thickness $lx[z]$ and width $ly[z]$.

For this study, cost-related variables were excluded.

2.6.3. Deterministic Recurrence Relationships

The following deterministic recurrence relationships were obtained using the variables described:

First Level:

$$F_{nz}(H, dbh, Hb) = \text{MAX}\{R_u(Jz.kz, d_{min(i)}, d_{max(i)}) + F_{nz\text{-}Jz.kz}(\text{nz.kz} - \text{Jz.kz}, dbh, Hb)\}$$

$$R_u(Jz.kz, d_{min(i)}, d_{max(i)}) = \Sigma_{\text{w=1}}\, Q_{iuw}(Jz.kz, d_{min(i)}, d_{max(i)}).P_{iuw} - \Sigma_{\text{w=1}}\, \Sigma_{\text{y=1}}\, C_{yiuw}(Jz.kz, d_{min(i)}, d_{max(i)}), \text{ para u} \neq \text{saw lumber, ou}$$

$$R_u(Jz.kz, d_{min(i)}, d_{max(i)}) = 0, \text{ para } nz = 0$$

Second Level:

$$F_{\text{nx}}(nxkx) = \text{MAX}\{G_{ny}(NY.ky, nx.kx, nx.kx - Lx[z]) + F_{nx-Lx[z]/kx}(nx.kx - Lx[z] - \text{skx})\}$$

$$\text{Lx[z]} \in \text{S}_1, \text{S}_1 = Lx[z]/z \in \text{Z}$$

$$0 \leq nx \leq NX; \text{F}_0 = 0$$

Third Level:

$$G_{ny}(ny.ky, nx.kx, nx.kx - Lx[z]) = \text{MAX}\{\text{V(w}, ny.ky, nx.kx, Lx[z], Ly[z]) + q_{ny\text{-}\,Ly[z]/ky\text{-}sky}(ny.kyLy[z] - sky)\}$$

$$Ly[z] \in \text{S}_2, \text{S}_2 = Ly[z]/z \in \text{Z}$$

$$0 \leq nx \leq NY; \text{G}_0 = 0$$

The structure of the plantation was detailed by diameter classes, specifying the *dbh* of the class mark, the height (H) and the number of individuals per hectare (trees ha^{-1}). The H of each diameter class was estimated using the best hypsometric model. The best profile equations were entered for each plantation, with d and h as dependent variables.

Because *C. cateniformis* wood is mainly used in the sawmill industry, simulations were performed for round and sawn wood. Surveys were conducted with the main sawmills in the city of Iquitos to determine the wood dimensions most commonly marketed. The simulations for round wood-covered log lengths from 1.83 to 3.05 mfv and a cutting yield of 90% were considered. In the case of sawn lumber, widths from 10.16 to 25.40 cm and thicknesses from 2.54 to 5.08 cm were considered, and the cutting width was 4 mm.

3. Results

3.1. Diametric Distribution Structure and Diameter–Height Relationship

The specific diameter classes (5 cm intervals) for the seven plantations evaluated are shown in Figure 3a. The diameters were normally distributed, ranging from 7.5 to 102.5 cm. Plantation P-1 included five classes, with the 17.5 cm class containing the highest number of trees (189 trees ha^{-1}), followed by the 22.5 cm class (156 trees ha^{-1}) and the 27.5 cm class (89 trees ha^{-1}). Plantation P-2 included seven classes, with the 22.5 cm class containing most trees (58 trees ha^{-1}) and frequencies decreasing for the lower and higher classes. Plantation P-3 included 12 classes covering a wide range of diameters, each with a low density, and a maximum of eight trees ha^{-1} were recorded in the 42.5 and 47.5 cm classes. Plantation P-4 included 10 classes, with the 52.5 and 62.5 cm classes having the highest number of individuals (13 trees ha^{-1}). Plantation P-5 also presented a wide variety of diameters, with 17 diameter classes, but all classes had low counts, with a peak of 8 trees ha^{-1} in the 22.5, 32.5 and 42.5 cm classes. Plantation P-6 had 10 classes, with the 32.5 cm class including the largest number of individuals (35 trees ha^{-1}), followed by the 27.5 cm class with 30 trees ha^{-1}. Plantation P-7 had 15 classes; the count is notable in the 27.5, 32.5 and 42.5 cm classes, which included 49, 34 and 41 trees ha^{-1}, respectively, indicating a high density and a diameter range that reflects mature individuals.

The selection criteria for the hypsometric models were based on a higher R^2, indicative of greater explanatory power and consistent data behavior, with the red regression lines representing the models (Figure 3b). Model fits were statistically significant, explaining the variability in the height data from 14.23 to 72.25%. The models included a logarithmic function, and the predictive variables were the inverse of the *dbh* (P1, P2, P4, P5 and P6) or its logarithm (P3 and P7). Plantation P-1 included trees of 8.05 to 16.50 m in total height, on average, for diameter classes of 7.5 and 27.5 cm, respectively. In plantation P-2, the total heights of trees were, on average, 8.12 to 18.76 m for the diameter classes 7.5 and 37.5 cm, respectively. In plantation P-3, the total heights of the trees were, on average, 18.03 to 32.03 m for diameter classes 17.5 and 72.5 cm, respectively. In plantation P-4, the total heights of the trees were, on average, 23.00 to 30.08 m for diameter classes 22.5 and 87.5 cm, respectively. In plantation P-5, the total heights of the trees were, on average, 15.02 to 31.06 m for diameter classes 17.5 and 102.5 cm, respectively. In plantation P-6, the total heights of the trees were, on average, 6.62 to 23.23 m for diameter classes 7.5 and 67.5 cm, respectively. Finally, in plantation P-7, the total heights of trees were, on average, 14.43 to 42.16 m for diameter classes of 12.5 and 97.5 cm, respectively. The horizontal (diametric classes) and vertical (heights) structures varied between plantations.

3.2. Taper Modeling

Table 5 shows statistical estimates for various models applied to different plantations (P-1 to P-7) to analyze certain coefficients across equations. For models such as Cielito I, Cielito II, Clutter, Kozak, Ormerod and Garay, statistically significant fits were obtained for all their parameters ($p < 0.05$). Models such as Demaerschalk, Amidon and COFORD e IFER had more non-significant values, suggesting limited applicability or less reliable parameter estimates for the specific plantations (e.g., P3, P5 and P6).

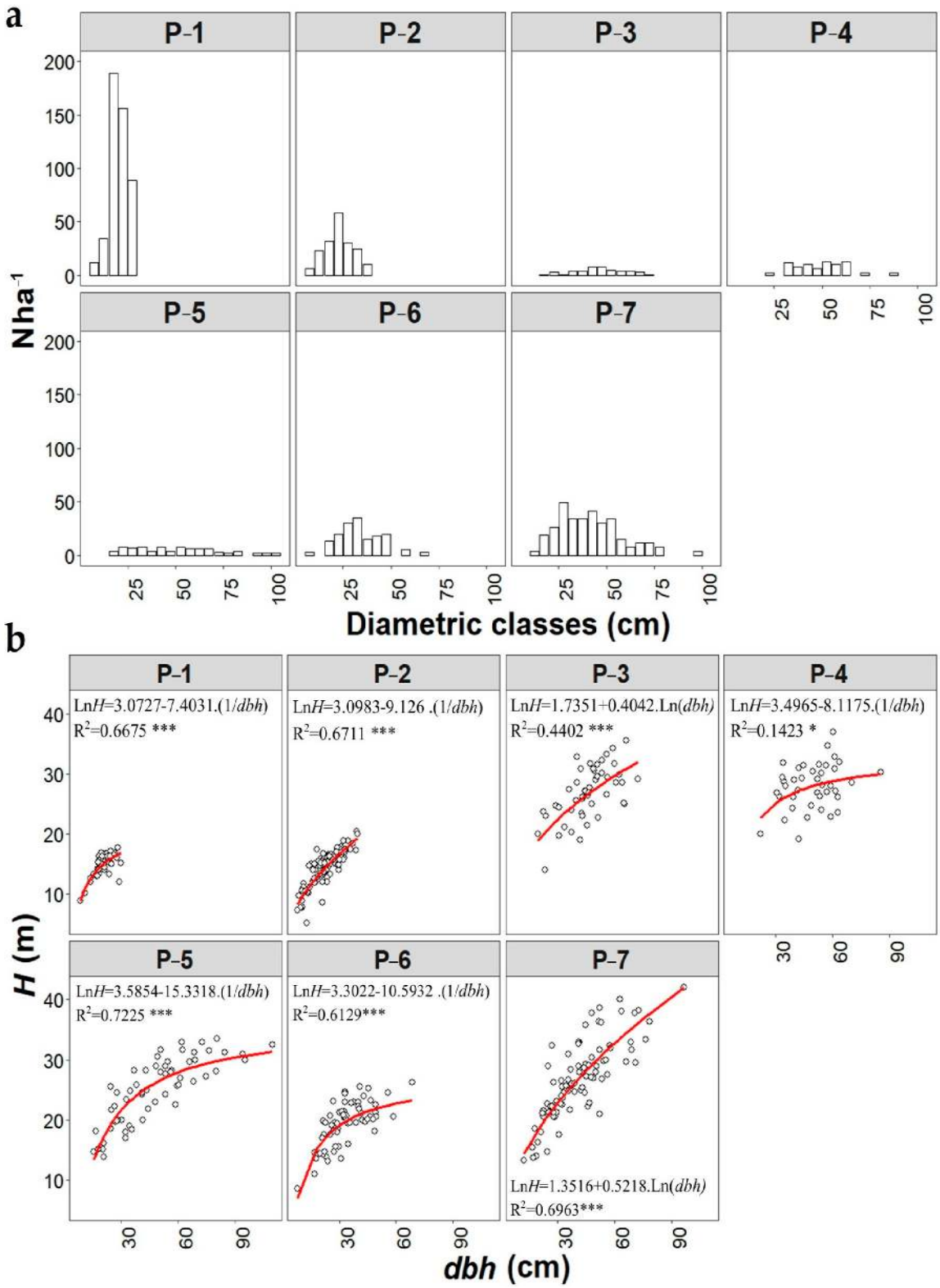

Figure 3. Diameter distribution (**a**) and height-diameter curves (**b**) for *Cedrelinga cateniformis* plantations. *dbh* denotes the diameter at breast height at 1.3 m above ground level in cm; *H* is the total height of the tree in m; and log denotes the natural logarithm. Circles indicate field observations, and the red line represents the fitted hypsometric model. * = $p < 0.05$, *** = $p < 0.0001$.

Table 5. Coefficients and significance of profile models for *Cedrelinga cateniformis* distributed in different plantation types in the Peruvian Amazon.

Plantation	Equation	Model	β_0	β_1	β_2	β_3	β_4
P-1	(1)	Cielito I	-	2.6367 ***	−6.4578 ***	5.3099 ***	-
	(2)	Cielito II	1.6473 ***	−10.5955 ***	42.5310 ***	−79.6238 ***	52.9715 ***
	(3)	Clutter	2.6951 ***	0.9880 ***	−1.3552 ***	1.0496 ***	-
	(4)	Amidon	-	1.0294 ***	−0.0719 ns	-	-
	(5)	Kozak	1.4253 ***	−4.3401 ***	4.3352 ***	-	-
	(6)	Demaerschalk	0.4306 ***	0.9880 ***	−0.6776 ***	0.5248 ***	-
	(7)	Ormerod	-	1.0065 ***	-	-	-
	(8)	Cervera	1.0086 ***	−4.2973 ***	17.3195 ***	−36.4661 ***	26.6667 ***
	(9)	Garay	1.4083 ***	−0.7795 ***	−1.5982 ***	0.5109 ***	-
	(10)	COFORD e IFER	-	−0.5955 ***	0.7755 **	0.0003 ***	-
P-2	(1)	Cielito I	-	2.1966 ***	−5.6452 ***	5.0686 ***	-
	(2)	Cielito II	1.8447 ***	−12.5610 ***	48.8622 ***	−85.6369 ***	52.4065 ***
	(3)	Clutter	1.9441 ***	0.9577 ***	−1.2649 ***	1.1284 ***	-
	(4)	Amidon	-	1.0566 ***	−0.1645 ***	-	-
	(5)	Kozak	1.5313 ***	−4.4711 ***	3.9217 ***	-	-
	(6)	Demaerschalk	0.2887 ***	0.9577 ***	−0.6325 ***	0.5642 ***	-
	(7)	Ormerod	-	1.0381 ***	-	-	-
	(8)	Cervera	1.1122 ***	−3.9432 ***	7.0278 ***	−3.282 ns	−2.6621 ns
	(9)	Garay	1.4327 ***	−1.9923 ***	−0.5140 **	0.4968 *	-
	(10)	COFORD e IFER	-	−0.4620 ***	0.0704 **	0.0252 ***	-
P-3	(1)	Cielito I	-	1.5211 ***	−3.5346 ***	3.2859 ***	-
	(2)	Cielito II	1.3918 ***	−8.7808 ***	36.9321 ***	−72.7176 ***	49.83182 ***
	(3)	Clutter	1.6416 ***	0.8479 ***	−1.1331 ***	1.1862 ***	-
	(4)	Amidon	-	1.0120 ***	−0.1213 *	-	-
	(5)	Kozak	1.2355 ***	−3.4404 ***	2.9894 ***	-	-
	(6)	Demaerschalk	0.2153 ***	0.8479 ***	−0.5665 ***	0.5931 ***	-
	(7)	Ormerod	-	1.1592 ***	-	-	-
	(8)	Cervera	1.0381 ***	−5.0939 ***	21.9141 ***	−47.6002 ***	35.3879 ***
	(9)	Garay	1.2006 ***	−1.9589 ***	−0.5274 **	0.6099 **	-
	(10)	COFORD e IFER	-	−0.7457 ns	0.0397 ns	0.0188 ***	-
P-4	(1)	Cielito I	-	2.2812 ***	−5.5187 ***	4.5587 ***	-
	(2)	Cielito II	1.5037 ***	−10.30521 ***	40.5168 ***	−68.6426 ***	39.9844 ***
	(3)	Clutter	1.9809 ***	1.0244 ***	−1.0921 ***	0.8755 ***	-
	(4)	Amidon	-	1.0177 ***	−0.1385 *	-	-
	(5)	Kozak	1.2471 ***	−3.4367 ***	3.0283 ***	-	-
	(6)	Demaerschalk	0.2969 *	1.0244 ***	−0.5461 ***	0.4378 ***	-
	(7)	Ormerod	-	0.8548 ***	-	-	-
	(8)	Cervera	1.1136 ***	−6.8880 ***	30.0872 ***	−56.0962 ***	35.0389 ***
	(9)	Garay	1.5299 **	−1.7740**	−0.5223 **	0.3101 **	-
	(10)	COFORD e IFER	-	−2.9905 ***	0.1342 ***	0.0062 ***	-
P-5	(1)	Cielito I	-	0.9199 ***	−1.4577 **	1.8637 ***	-
	(2)	Cielito II	1.4499 ***	−7.7048 ***	28.5881 ***	−49.9187 ***	29.8572 ***
	(3)	Clutter	1.1555 ***	0.8918 ***	−0.9449 ***	1.0684 ***	-
	(4)	Amidon	-	1.0465 ***	−0.1589 ***	-	-
	(5)	Kozak	1.2899 ***	−2.8793 ***	1.8474 ***	-	-
	(6)	Demaerschalk	0.0628 ns	0.8919 ***	−0.4724 ***	0.5342 ***	-
	(7)	Ormerod	-	0.9632 ***	-	-	-
	(8)	Cervera	1.1108 ***	−4.1757 ***	14.6614 ***	−27.9422 ***	18.0384 ***
	(9)	Garay	1.1712 ***	−4.3455 **	−0.2340 **	0.7972 ***	-
	(10)	COFORD e IFER	-	−0.2177 ns	0.0031 ns	0.0048 ns	-
P-6	(1)	Cielito I	-	0.7490 ***	−1.6084 **	2.2074 ***	-
	(2)	Cielito II	1.4639 ***	−7.8082 ***	28.6149 ***	−53.6171 ***	35.7454 ***
	(3)	Clutter	1.7447 ***	0.9034 ***	−1.3836 ***	1.3603 ***	-
	(4)	Amidon	-	1.0244 ***	−0.2743 ***	-	-
	(5)	Kozak	1.3144 ***	−3.4834 ***	2.6341 ***	-	-
	(6)	Demaerschalk	0.2417**	0.9034 ***	−0.6918 ***	0.6802 ***	-
	(7)	Ormerod	-	1.2869 ***	-	-	-
	(8)	Cervera	1.0497 ***	−4.0688 ***	14.2263 ***	−30.5012 ***	23.0377 ***
	(9)	Garay	1.2066 ***	−4.4049 ***	−0.2582 ***	0.7581 **	-
	(10)	COFORD e IFER	-	−1.2023 ns	0.0318 ns	0.0438 ***	-
P-7	(1)	Cielito I	-	1.6700 ***	−3.8591 ***	3.5137 ***	-
	(2)	Cielito II	1.4592 ***	−8.9219 ***	32.6118 ***	−53.6524 ***	30.6442 ***
	(3)	Clutter	1.8009 ***	1.0317 ***	−1.1722 ***	0.9822 ***	-
	(4)	Amidon	-	1.0231 ***	−0.1103 ***	-	-
	(5)	Kozak	1.2640 ***	−3.2419 ***	2.5407 ***	-	-
	(6)	Demaerschalk	0.2555 ***	1.0317 ***	−0.5861 ***	0.4911 ***	-
	(7)	Ormerod	-	0.9377 ***	-	-	-
	(8)	Cervera	1.0818 ***	−5.2557 ***	19.3922 ***	−34.1951 ***	20.7376 ***
	(9)	Garay	1.3510 ***	−3.9110 ***	−0.2219 **	0.4214 *	-
	(10)	COFORD e IFER	-	−0.5717 ***	0.1017 ***	0.0055 ***	-

ns = not significant at the 0.05 significance level, * = $p < 0.05$, ** = $p < 0.001$, *** = $p < 0.0001$.

Analysis of model performance across plantations (P-1 to P-7) is summarized in Table 6. In plantation P-1, the Cielito II and Cervera models stand out, with the highest R^2_{adj} values

of 0.953 and 0.951, respectively, indicating a strong model fit. Both models also present high values for $r_{Y\hat{Y}}$ (0.980 and 0.980) and low RMSE values (1.299 and 1.337), suggesting high prediction accuracy. Cielito II presents the lowest RMSE% (7.041%), while Garay reaches an equally low RMSE% (7.592%). Likewise, the Cielito II and Cervera models present the lowest values for the AIC (46.996 and 46.824). The Ormerod and COFORD and IFER models show higher values of Bias and Bias%, suggesting some systematic errors in their predictions. Cielito II and Cervera models present good statistical indicators, which makes them strong candidates for modeling the profile in this plantation.

For plantation P-2, the Garay model yielded the highest R^2_{adj} (0.967), followed by Cielito II (0.965), both with excellent fits, with a $r_{Y\hat{Y}}$ of 0.984. Garay also yielded the lowest RMSE, RMSE% and AIC, with values of 1.603, 8.074% and 85.376, respectively, demonstrating precise predictions. Cielito II and Cervera also perform well with relatively low RMSE values. However, COFORD and IFER have a high bias (−8.110%), indicating a notable lack of systematic prediction. Overall, the Garay and Cielito II models were the most reliable for modeling the screw profile in this plantation.

In plantation P-3, the Garay model again performed well, with a high R^2_{adj} and $r_{Y\hat{Y}}$ (0.888 and 0.943) and the lowest RMSE (4.190), RMSE% (11.206%) and AIC (135.688). The Cielito I and Cervera models followed closely with good fit and moderate RMSE values. Models such as Amidon and Demaerschalk yielded higher RMSE%, indicating less accurate predictions. The COFORD and IFER models also led to slightly higher Bias%. The Garay model was the most effective for profile modeling.

In plantation P-4, the Cielito II and Cervera models produced good results with high values of R^2_{adj} (0.946 and 0.943) and $r_{Y\hat{Y}}$ (0.978 and 0.976), low RMSE values and low AIC scores, suggesting strong fit and accuracy. Garay also yielded a relatively low AIC (85.692), although only slightly lower than that of Cielito II and Cervera. Models such as Kozak, Cielito I, Clutter and Demaerschalk yielded higher Bias% and AIC values, indicating systematic error. The Cielito II and Cervera models were the most accurate for this plantation.

In plantation P-5, Garay yielded high R^2_{adj} and $r_{Y\hat{Y}}$ values (0.942 and 0.971) with low RMSE and AIC (4.971 and 206.387), demonstrating a robust fit and accuracy. The Amidon and Demaerschalk models also performed well, but Amidon yielded the lowest AIC (209.608) among the models. COFORD and IFER yielded a high AIC (216,488), suggesting that it is less optimal for this plantation. The Garay and Amidon models appear to be the best choices for this plantation due to their combination of high fit and low AIC.

The Garay model yielded the best results for plantation P-6, with the highest R^2_{adj} and $r_{Y\hat{Y}}$ values (0.951 and 0.976), the lowest RMSE and AIC (3.257 and 99.231). Demaerschalk also produced good results, but with a slightly higher RMSE%. The Amidon and COFORD and IFER models yielded high RMSE% and Bias% values, indicating a notable prediction error. The statistical indicators showed that the Gary model performed best for this plantation.

For plantation P-7, the Garay model again yielded the highest R^2_{adj} and $r_{Y\hat{Y}}$ values (0.963 and 0.982), along with the lowest RMSE (3.610) and the lowest AIC (238.586), making this one of the best models. Cervera yielded high fit and precision with values for R^2adj, RMSE and AIC of 0.951, 4.118 and 260.013, respectively. The Amidon, Clutter, and COFORD and IFER models yielded higher RMSE, RMSE% and AIC values, indicating less reliable predictions. The Garay model again provided the best fits, reinforcing its effectiveness.

Table 6. Model performance metrics for *Cedrelinga cateniformis* in different types of plantations in the Peruvian Amazon.

Plantation	Model	Equation	R^2_{adj}	$r_{Y\hat{Y}}$	RMSE	RMSE%	Bias	Bias%	AIC
P-1	Cielito I	(1)	0.924	0.964	1.680	9.105	−0.228	−1.238	79.378
	Cielito II	(2)	0.953	0.980	1.299	7.041	−0.261	−1.415	46.996
	Clutter	(3)	0.890	0.949	2.013	10.908	−0.390	−2.115	103.555
	Amidon	(4)	0.897	0.950	11.277	61.123	−0.406	−2.202	101.193
	Kozak	(5)	0.910	0.956	1.838	9.962	−0.232	−1.258	87.421
	Demaerschalk	(6)	0.890	0.949	2.012	10.904	−0.389	−2.110	103.501
	Ormerod	(7)	0.881	0.949	2.131	11.548	−0.786	−4.261	105.181
	Cervera	(8)	0.951	0.980	1.337	7.245	−0.292	−1.581	46.824
	Garay	(9)	0.948	0.978	1.401	7.592	−0.491	−2.663	55.080
	COFORD e IFER	(10)	0.872	0.949	2.185	11.845	−0.972	−5.268	114.572
P-2	Cielito I	(1)	0.933	0.968	2.287	11.520	0.326	1.641	142.193
	Cielito II	(2)	0.965	0.984	1.642	8.273	0.281	1.414	91.282
	Clutter	(3)	0.944	0.973	2.079	10.476	−0.303	−1.525	127.003
	Amidon	(4)	0.948	0.974	10.170	51.234	−0.146	−0.736	121.762
	Kozak	(5)	0.923	0.963	2.453	12.358	0.267	1.346	149.415
	Demaerschalk	(6)	0.944	0.973	2.079	10.474	−0.302	−1.523	126.983
	Ormerod	(7)	0.932	0.974	2.313	11.652	−1.009	−5.084	138.017
	Cervera	(8)	0.956	0.978	1.838	9.262	−0.066	−0.332	104.790
	Garay	(9)	0.967	0.984	1.603	8.074	−0.290	−1.462	85.376
	COFORD e IFER	(10)	0.914	0.975	2.589	13.044	−1.610	−8.110	162.046
P-3	Cielito I	(1)	0.878	0.940	4.355	11.646	0.766	2.050	139.066
	Cielito II	(2)	0.871	0.938	4.426	11.838	0.765	2.046	142.501
	Clutter	(3)	0.857	0.929	4.684	12.527	0.410	1.096	145.464
	Amidon	(4)	0.864	0.931	12.926	34.570	0.486	1.300	144.354
	Kozak	(5)	0.874	0.938	4.417	11.812	0.736	1.969	136.309
	Demaerschalk	(6)	0.857	0.929	4.686	12.532	0.425	1.137	145.496
	Ormerod	(7)	0.866	0.932	4.604	12.315	−0.505	−1.351	137.962
	Cervera	(8)	0.876	0.939	4.372	11.694	0.639	1.709	137.423
	Garay	(9)	0.888	0.943	4.190	11.206	−0.148	−0.395	135.688
	COFORD e IFER	(10)	0.861	0.932	4.644	12.422	−0.812	−2.173	144.721
P-4	Cielito I	(1)	0.897	0.956	5.287	12.972	1.827	4.483	99.681
	Cielito II	(2)	0.943	0.976	3.871	9.498	1.159	2.844	84.893
	Clutter	(3)	0.890	0.951	5.417	13.289	1.628	3.994	100.982
	Amidon	(4)	0.920	0.961	11.499	28.211	0.167	0.410	93.551
	Kozak	(5)	0.882	0.949	5.668	13.907	1.963	4.817	99.429
	Demaerschalk	(6)	0.890	0.951	5.417	13.290	1.631	4.001	100.985
	Ormerod	(7)	0.900	0.950	5.316	13.043	0.922	2.262	93.975
	Cervera	(8)	0.946	0.978	3.793	9.305	1.298	3.185	79.791
	Garay	(9)	0.940	0.973	4.078	10.004	1.196	2.935	85.692
	COFORD e IFER	(10)	0.919	0.963	4.706	11.547	−1.155	−2.834	93.413
P-5	Cielito I	(1)	0.922	0.962	5.768	14.458	1.216	2.983	224.620
	Cielito II	(2)	0.922	0.963	5.714	13.004	1.107	2.715	225.449
	Clutter	(3)	0.937	0.969	5.139	32.949	−0.429	−1.053	210.471
	Amidon	(4)	0.939	0.971	13.021	14.650	−1.058	−2.596	209.608
	Kozak	(5)	0.921	0.962	5.790	12.996	1.131	2.776	221.071
	Demaerschalk	(6)	0.937	0.969	5.136	13.693	−0.399	−0.978	210.397
	Ormerod	(7)	0.932	0.970	5.411	13.896	−1.695	−4.159	210.791
	Cervera	(8)	0.929	0.965	5.492	12.577	0.884	2.169	216.598
	Garay	(9)	0.942	0.971	4.971	3.561	−0.538	−1.321	206.387
	COFORD e IFER	(10)	0.931	0.970	5.398	3.150	1.407	3.452	216.488
P-6	Cielito I	(1)	0.928	0.968	3.950	14.266	1.245	4.347	113.808
	Cielito II	(2)	0.930	0.969	3.826	12.548	1.166	−0.388	113.400
	Clutter	(3)	0.947	0.974	3.365	49.295	−0.104	3.531	101.705
	Amidon	(4)	0.922	0.964	13.221	14.445	0.947	4.400	117.135
	Kozak	(5)	0.930	0.969	3.874	12.543	1.180	−0.360	108.341
	Demaerschalk	(6)	0.947	0.974	3.364	13.487	−0.097	−2.766	101.675
	Ormerod	(7)	0.941	0.972	3.617	13.985	−0.742	3.136	101.157
	Cervera	(8)	0.934	0.970	3.751	12.144	0.841	0.558	107.895
	Garay	(9)	0.951	0.976	3.257	12.652	0.150	1.128	99.231
	COFORD e IFER	(10)	0.947	0.976	3.393	16.136	0.303	2.243	102.325
P-7	Cielito I	(1)	0.946	0.974	4.328	12.796	0.602	1.696	270.866
	Cielito II	(2)	0.949	0.977	4.191	13.721	0.556	−1.211	267.143
	Clutter	(3)	0.942	0.971	4.494	40.121	−0.397	−2.610	277.568
	Amidon	(4)	0.943	0.973	13.140	12.957	−0.855	1.592	276.449
	Kozak	(5)	0.949	0.975	4.243	13.719	0.521	−1.208	263.360
	Demaerschalk	(6)	0.942	0.971	4.493	14.183	−0.396	−1.699	277.537
	Ormerod	(7)	0.939	0.969	4.645	12.573	−0.556	0.513	277.456
	Cervera	(8)	0.951	0.976	4.118	11.023	0.168	−0.244	260.013
	Garay	(9)	0.963	0.982	3.610	13.962	−0.080	−5.459	238.586
	COFORD e IFER	(10)	0.940	0.975	4.572	0.000	−1.788	0.000	280.660

R^2_{adj} represents the coefficient of determination; $r_{Y\hat{Y}}$ denotes the coefficient of correlation; RMSE is the root mean square error; RMSE% is the percentage root mean square error; Bias%: denotes the percentage bias; and AIC is the Akaike Information Criterion.

In general, the Cielito II, Cervera and Garay models yielded lower RMSE and AIC values across different plantations and with consistently high adjusted R^2 values and $r_{Y\hat{Y}}$, showing their strong prediction accuracy and further supporting their effectiveness in model selection. The Ormerod and COFORD and IFER models yielded relatively higher biases in certain plantations, potentially indicating systematic errors in their predictions.

The relative error (RE %) is shown in Figure 4 as a function of the estimated diameter (*d*) in plantations P-1 to P-7 for the Cielito II, Cervera and Garay models. The model errors showed similar trends, with higher estimation errors for small diameters and lower errors for larger diameters. The precision remained around zero for most observations; in plantations P-1 and P-4, the lowest RE, on average, was obtained for the Cielito II model, with values of −0.664 and 5.898%, respectively. In plantation P-2, the lowest error was found for the Cervera model, with 0.420%. Finally, in plantations P-3, P-5, P-6 and P-7, the Garay model yielded the lowest RE value, on average, with values of 1.122, 0.329, 1.299, −0.929 and −0.203%, respectively. In general, the residual analysis reinforced the good performance of the Cielito II, Cervera and Garay models at different relative heights, consistent with their high R^2adj values and low RMSE.

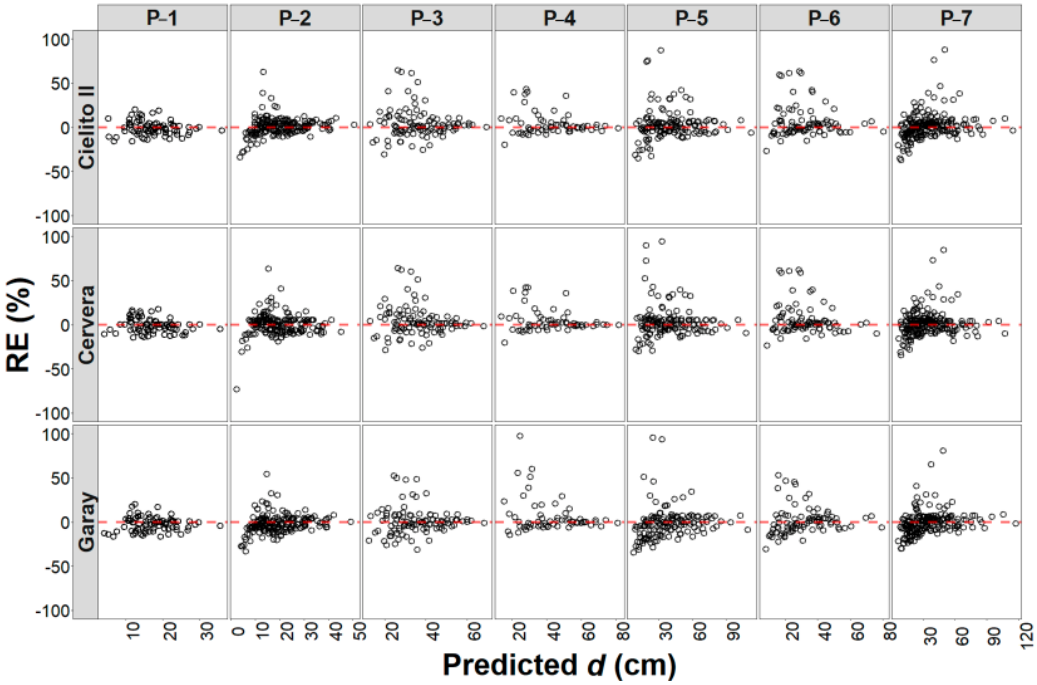

Figure 4. Evaluation of the Residue Percentage (RE%) based on the expected diameter (*d*) by plantation type for *Cedrelinga cateniformis* in the Peruvian Amazon. Circles denote the residuals, while the red line indicates zero error.

To improve the model selection analysis, biological realism was also evaluated by assessing the behavior and patterns of the model in relation to the stem characteristics of the species (Figure 5). The formation of the curve shown in Graph 5 of relative height versus diameter reflects the natural growth of *C. cateniformis*, with more pronounced diameter growth at the base of the tree and a gradual decrease in diameter growth as height increases. The Cielito II and Cervera models correctly represented the relationship between d/dbh and h/H at the base of the stem; however, deviations were observed in the upper sections. Analysis of the different models in plantations P-1 to P-7 indicates that Garay's model most closely matches the biological realism of the species in question. Although some models, such as Cielito II in P-1 and Cervera in P-4, performed well, with high adjusted R^2 values, low RMSE and minimal Bias%, Garay's model consistently achieved high accuracy while

reflecting the profile patterns of the species, steadily decreasing in diameter as h increases. For example, in plantations P-2, P-3, P-5, P-6 and P-7, Garay's model not only provides the highest adjusted R^2 values, ranging from 0.888 to 0.963, but also maintains a low RMSE and Bias%, suggesting accurate prediction with minimal error. The strong alignment of this model with both statistical metrics and biological characteristics of the species makes it the most reliable choice for all plantations, allowing consistent and ecologically sound predictions under various structural conditions for *C. cateniformis*.

For the practical visualization of the stem shape of *C. cateniformis* established in the plantations under study, the profile of the trees by diameter class was generated from the observed values (dispersion) and the predicted values (solid lines) using the Garay model (Figure 6). For example, in plantation P-1, the diameters of the sections of a tree with an average *dbh* of 8.4 cm, at 0.3, 2.0, 4.0 and 6.0 m in height, were 10.1, 8.0, 6.0 and 4.7 cm, respectively. Likewise, the diameters of sections of a tree with an average *dbh* of 29.7 cm, at 0.3, 2.0, 4.0, 6.0 and 8.4 m height, were 37.2, 27.0, 24.1, 23.1 and 18.4 cm, respectively. In plantation P-2, the diameters of the sections of a tree with an average *dbh* of 8.7 cm, at 0.3, 2.0, 4.0 and 6.0 m in height, were 10.9, 7.6, 6.5 and 5.6 cm, respectively. The diameters of sections of a tree with an average *dbh* of 39.1 cm, at 0.3, 4.0, 8.0, 12.0 and 14.0 m in height, were 49.1, 36.4, 27.9, 14.5 and 12.4 cm, respectively. Finally, in plantation P-7, the diameters of sections of a tree with an average *dbh* of 16.6 cm, at 0.3, 3.0 and 6.0 m in height, were 18.0, 12.3 and 9.9 cm, respectively. Likewise, the diameters of a tree with an average *dbh* of 96.9 cm, at 0.3, 6.0, 12.0, 18.0 and 24.0 m height, were 118.9, 80.7, 72.4, 46.4 and 26.7 cm, respectively.

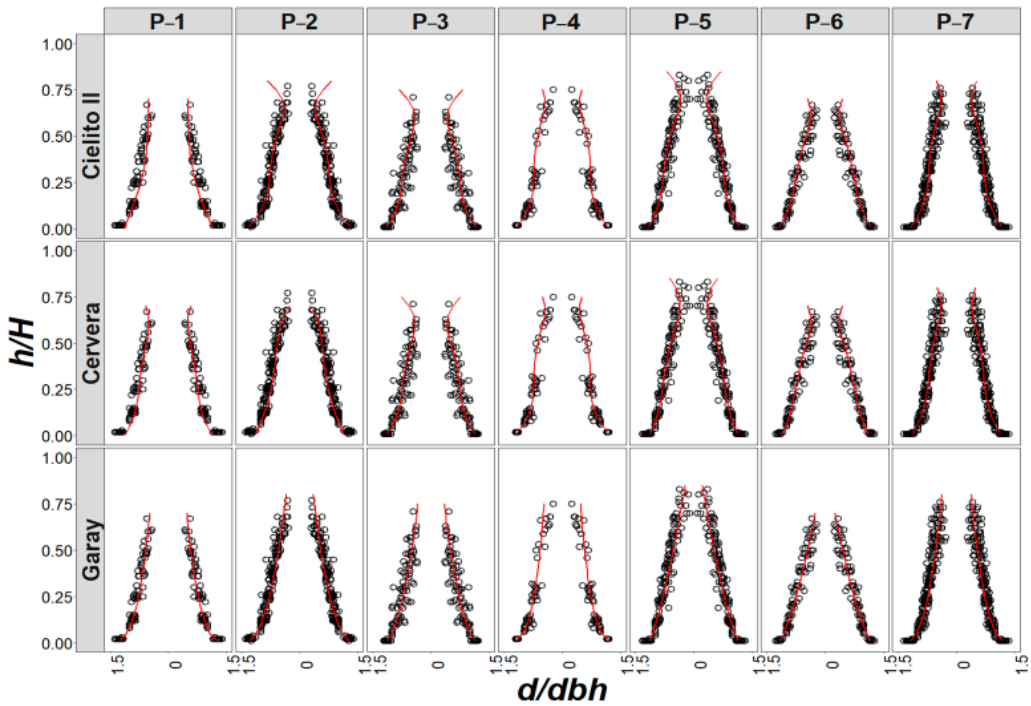

Figure 5. Relationship between relative height (h/H) and relative diameter (d/dbh) across different locations and plantations. Circles represent the field observations (relatives) and the red line the profile model functions.

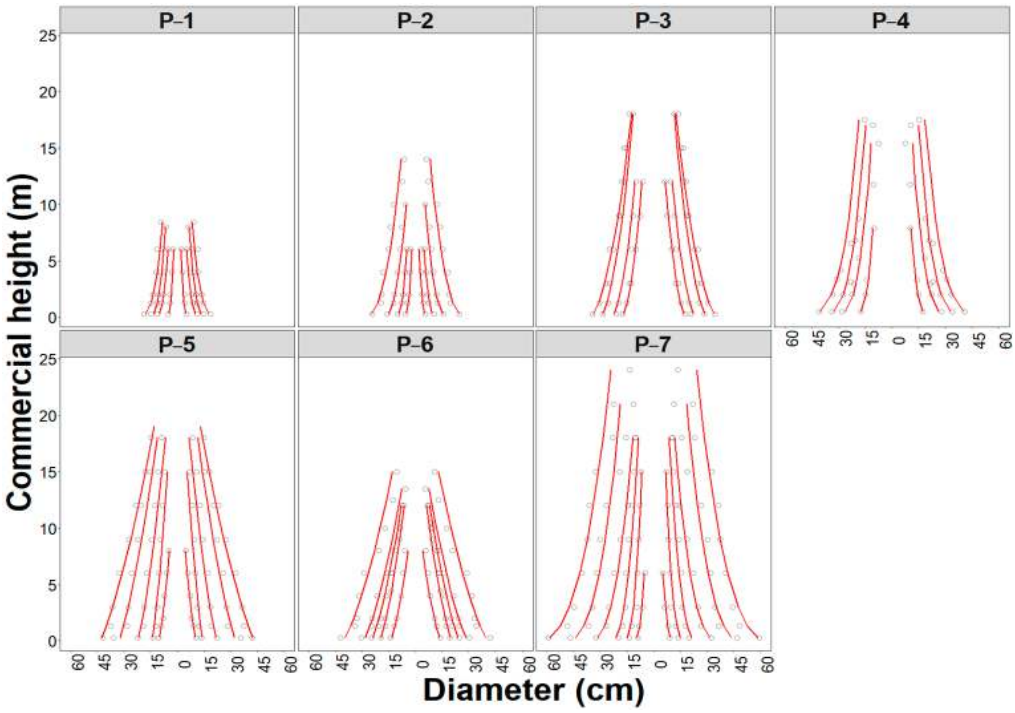

Figure 6. Observed (scatter) and predicted (solid lines) profiles by diameter class of various trees using the Garay model.

3.3. Model Optimization

3.3.1. Optimization of Log Cutting

Once the height–diameter relationship model was established, volumes were estimated for the diameter classes defined by the dataset. The standing volumes of trees were 33.1137, 29.8444, 70.2215, 181.9544, 205.2809, 98.5093 and 564.5432 m^3ha^{-1} for plantations P-1, P-2, P-3, P-4, P-5, P-6 and P7, respectively. Table 7 and Figure 7 show the distribution of the quantity (N ha^{-1}) and volume (m^3ha^{-1}) of log across different diameter classes (cm) for various plantations (P-1 to P-7) using specific log lengths (1.83, 2.13, 2.44, 2.74 and 3.05 m). These lengths were chosen as the optimal combinations for producing log products, maximizing efficiency in the cutting process. All dimensions were established starting from a minimum diameter of 20 cm, which was identified as the optimal solution for maximizing log yield.

Plantation P-1 yielded relatively low volumes of wood, with lengths of 1.83 and 2.13 m corresponding to 156 and 178 logs, which, in total, represented 11.5271 and 18.2752 m^3ha^{-1}, respectively (Table 7). Similarly, low volumes distributed in 243 logs containing 26.8600 m^3ha^{-1} were recorded in plantation P-2. Plantation P-3 yielded a high volume of logs of lengths of 2.13 and 2.44 m, totaling 63,200 m^3ha^{-1} in 302 logs. Plantation P-4 yielded high volumes of logs of lengths of 2.13 and 2.44 m of 13.5088 and 49.4906 m^3ha^{-1}, respectively. This plantation had a total of 163,759 m^3ha^{-1} in 782 logs. In plantation P-5, the volumes were mainly comprised of logs of lengths of 2.74 and 3.05 m, with a total volume of 184,753 m^3ha^{-1} in 416 logs. Plantation P-6 yielded a total log volume of 88,659 m^3ha^{-1} comprised of a total of 450 logs of lengths 2.13 and 2.44 m. Plantation P-7 yielded the highest total volume (508,089 m^3ha^{-1} in 1712 logs), with significant quantities of lengths of 2.74 and 3.05 m of volumes of 126,4132 and 379,838 m^3ha^{-1}. The log length obviously increased with the age of the plantations, as older trees have larger dimensions (Figure 7).

A table is provided in Supplementary S2, outlining the log optimization in further detail. This table includes the position or range of measurement for each log segment, along

with the total volume and the recovered volume, as determined by the best optimized cutting strategies, showing how the cuts were made to maximize the volume recovered while minimizing waste.

Table 7. Volumes of log-by-length classes across different types of *Cedrelinga cateniformis* plantations in the Peruvian Amazon.

Plantation	Log Lengths (m)					Total ($m^3 ha^{-1}$)
	1.83	2.13	2.44	2.74	3.05	
P-1	11.5271	18.2752				29.8023
P-2	10.7798	16.0802				26.8600
P-3	0.2006	13.5088	49.4906			63.2000
P-4		79.4685	84.2906			163.7591
P-5				40.0938	144.6596	184.7534
P-6		34.8302	53.8283			88.6585
P-7	1.8374			126.4132	379.8380	508.0886

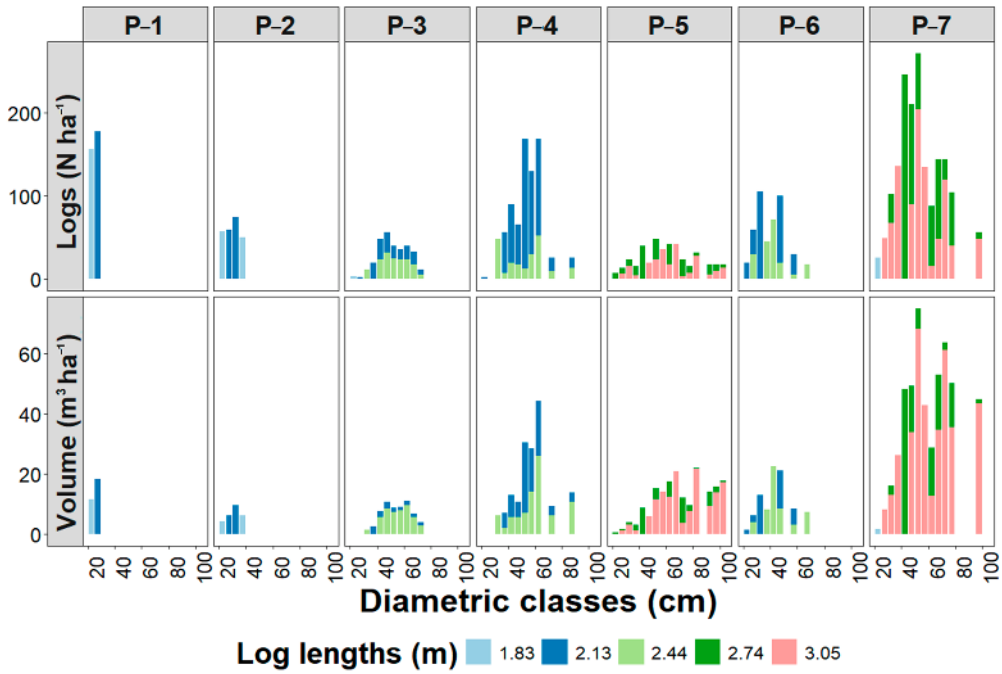

Figure 7. Distribution of log quantity (N ha^{-1}) and volume ($m^3 ha^{-1}$) by diameter classes and lengths across different *Cedrelinga cateniformis* plantations in the Peruvian Amazon.

3.3.2. Optimization of Sawn Lumber Cutting

The volumes of sawn lumber based on piece dimensions by log length classes for each plantation (P-1 to P-7) are shown in Table 8. Lumber yields varied among plantations, with 51.2, 57.3, 61.0, 63.7, 62.4, 54.7 and 62.3% for P-1, P-2, P-3, P-4, P-5, P-6 and P7, respectively. The yields also varied between diametric classes, with 46.2% in the 22.5 cm class and 68.4% in the 117.5 cm class.

In plantation P-1, the wood pieces measured 10.16 × 2.54 cm, 10.16 × 3.81 cm, 10.16 × 5.08 cm, 17.78 × 2.54 cm and 17.78 × 3.81 cm, distributed in lengths of 1.83 m and 2.13 m. Logs of dimensions 17.78 × 3.81 cm yielded the highest volume, totaling 6.3904 $m^3 ha^{-1}$ (38.1%) in 490 pieces of wood. Altogether, this plantation accumulated a volume of 16.7551 $m^3 ha^{-1}$ in 1781 pieces (Table 8 and Figure 8).

A wider range of dimensions was included in plantation P-2, with additional pieces measuring 25.40 × 2.54 cm and 25.40 × 3.81 cm. Volumes were distributed in lengths of 1.83 m and 2.13 m, with the 10.16 × 5.08 cm dimension yielding the largest sawn volume, with 5.7408 $m^3 ha^{-1}$ (35.63%) in 563 pieces; the total wood volume was 16.1079 $m^3 ha^{-1}$ in 1492 pieces (Table 8 and Figure 8).

Table 8. Volume of sawn lumber by length classes across different *Cedrelinga cateniformis* plantations in the Peruvian Amazon.

Plantation	Dimensions of Pieces (cm) (Width × Thickness)	Log Lengths (m)					Total (m^3ha^{-1})
		1.83	2.13	2.44	2.74	3.05	
P-1	10.16 × 2.54		1.4360				1.4360
	10.16 × 3.81	1.0957	3.6378				4.7335
	10.16 × 5.08	1.4417	1.9147				3.3563
	17.78 × 2.54		0.8388				0.8388
	17.78 × 3.81	3.8403	2.5501				6.3904
							16.7551
P-2	10.16 × 2.54	0.2772	0.6992				0.9764
	10.16 × 3.81	0.8990	0.4496				1.3486
	10.16 × 5.08	1.9222	3.8186				5.7408
	17.78 × 2.54	0.2429	0.2828				0.5257
	17.78 × 3.81	1.9201	1.1461				3.0662
	17.78 × 5.08	0.3239	2.4506				2.7745
	25.40 × 2.54	0.1162	0.6763				0.7925
	25.40 × 3.81	0.8832					0.8832
							16.1079
P-3	17.78 × 3.81	0.0369	2.9656	6.2856			9.2881
	17.78 × 5.08	0.0486	3.1103	12.1142			15.2732
	25.40 × 3.81		1.1513	8.3606			9.5119
	25.40 × 5.08		0.4328	6.8483			7.2812
							41.3542
P-4	17.78 × 5.08		10.9310	10.6182			21.5492
	17.78 × 5.08		21.4519	17.5343			38.9862
	25.40 × 3.81		8.6141	7.8189			16.4330
	25.40 × 5.08		15.9871	11.8374			27.8246
							104.7930
P-5	17.78 × 3.81				5.1418	17.0269	22.1686
	17.78 × 5.08				9.7723	42.7021	52.4745
	25.40 × 3.81				5.1571	18.7229	23.8800
	25.40 × 5.08				4.5933	24.7129	29.3063
							127.8294
P-6	17.78 × 3.81		6.3752	7.3031			13.6783
	17.78 × 5.08		6.4092	12.3518			18.7609
	25.40 × 3.81		1.9531	4.9221			6.8752
	25.40 × 5.08		5.0044	7.5301			12.5345
							51.8490
P-7	17.78 × 3.81	0.3200			24.0686	43.6134	68.0020
	17.78 × 5.08	0.4211			25.5827	101.9507	127.9545
	25.40 × 3.81				12.8530	43.0687	55.9217
	25.40 × 5.08				15.1371	66.5855	81.7226
							333.6007

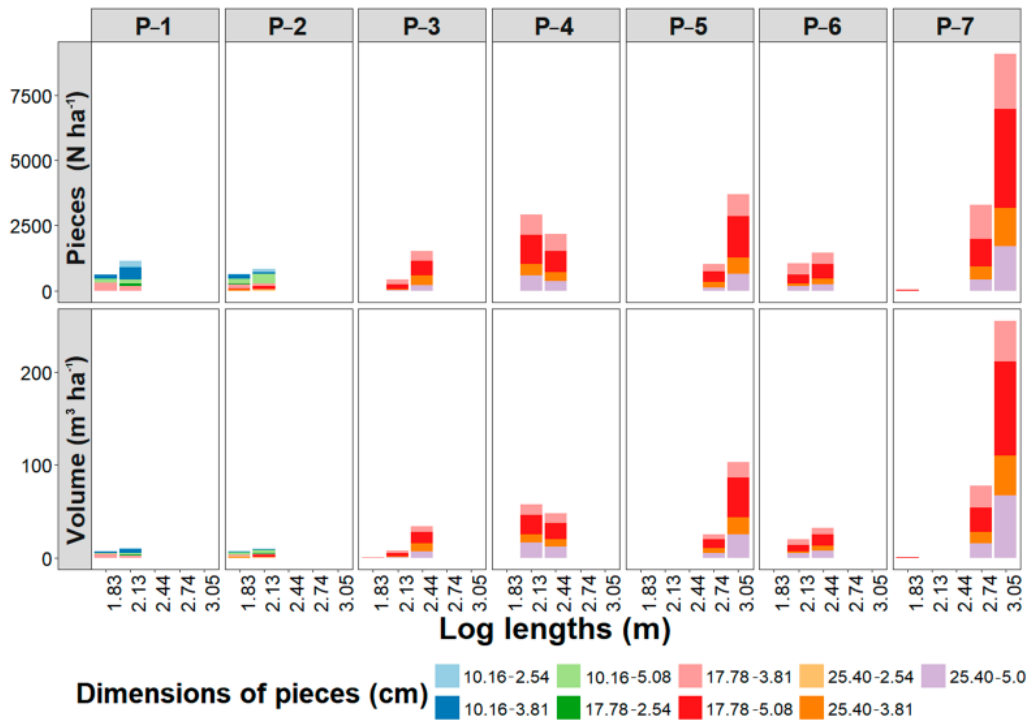

Figure 8. Distribution of volume and number of pieces by log lengths across different *Cedrelinga cateniformis* plantations in the Peruvian Amazon.

Plantation P-3 had larger volumes in longer lengths, such as 2.13 m and 2.44 m, with the most notable dimension being 17.78 × 5.08 cm with 15.2732 m^3ha^{-1}, which represented 36.9% in 729 pieces. This plantation yielded a total volume of 41.3542 m^3ha^{-1} in 1970 pieces, with a tendency towards longer pieces than in the previous plantations (Table 8 and Figure 8).

In plantation P-4, the wood volume increased significantly, reaching a total of 104.7930 m^3ha^{-1} in 5084 pieces. The predominant log lengths were 2.13 m and 2.44 m, with pieces of 17.78 × 5.08 cm and 25.40 × 5.08 cm contributing 38.9862 and 27.8246 m^3ha^{-1}, which represented 37.20 and 26.55% in 1950 and 973 pieces, respectively. This increase reflects the high availability of wood of larger dimensions and lengths (Table 8 and Figure 8).

In plantation P-5, the wood volume was concentrated in logs of lengths greater than 2.74 m and 3.05 m. In particular, logs of dimensions 17.78 × 5.08 cm and 25.40 × 5.08 cm yielded volumes of 52.4745 and 29.3063 m^3ha^{-1}, representing 41.05 and 22.935% in 1985 and 770 pieces, respectively; the total sawn volume was 127.8294 m^3ha^{-1} in 4695 pieces (Table 8 and Figure 8).

Plantation P-6 yielded timber more distributed in lengths of 2.13 m and 2.44 m, with the most representative pieces measuring 17.78 × 5.08 cm, reaching a total of 18.7609 m^3ha^{-1}, which represented 36.2% in 912 pieces. The total wood volume in the plantation was 51.8490 m^3ha^{-1} in 2534 pieces, indicating more moderate availability than in the other plantations (Table 8 and Figure 8).

Plantation P-7 yielded the highest total volume of timber, reaching 333.6007 m^3 in 12,419 pieces. The predominant lengths were 2.74 m and 3.05 m, with significant contributions from pieces measuring 17.78 × 5.08 cm and 25.40 × 5.08 cm, yielding volumes of 127.9545 m^3 and 81.7226 m^3, representing 38.36 and 24.50% in 4858 and 2154 pieces, respectively. This result reflects a high concentration of wood in larger dimensions and lengths (Table 8 and Figure 8).

In general, wood volumes varied significantly between plantations, with wood pieces of larger dimensions in plantations including mature, large individuals, such as plantations P-5 and P-7.

The optimal cutting configurations for each of the plantations (P-1 to P-7) across three different cutting patterns (Cut 1, Cut 2 and Cut 3) are shown in Figure 9. Each cut indicates the log length (L) and diameter (D), along with the specific dimensions of the pieces obtained from each log. These cuts were designed to maximize wood utilization based on the available length and diameter in each plantation.

In plantations P-1 and P-2, the optimized cuts were primarily for shorter lengths and smaller diameters, with pieces mainly of dimensions 10.16 × 3.81 cm, 10.16 × 5.08 cm and 17.78 × 3.81 cm. Plantation P-3 performed better than P-1 and P-2, as it produced larger components, including dimensions of 17.78 × 5.08 cm and 25.40 × 3.81 cm, particularly in Cut 2 and Cut 3. In plantations P-4 and P-5, the cuts were significantly more productive, with log lengths reaching up to 3.05 m and larger diameters (around 34–50 cm). This enabled the inclusion of larger pieces (e.g., 25.40 × 5.08 cm and 17.78 × 5.08 cm) n in optimized cuts. In plantatioP-6, optimized cutting took advantage of log lengths of up to 2.44 m and diameters of approximately 37 to 54 cm; this plantation allowed for versatile cutting configurations, yielding considerable amounts of pieces of dimensions of 25.40 × 3.81 cm and 17.78 × 5.08 cm. In P-7, the optimized cuts utilized logs up to 3.05 m in length and diameters greater than 50 cm in Cut 3. This enabled the extraction of large pieces of dimensions 25.40 × 5.08 cm and 17.78 × 5.08 cm in dense combinations.

Overall, the cutting configurations varied depending on the log length and diameter available in each plantation. The most productive plantations, such as P-7, P-5 and P-4, allowed for denser cutting configurations with larger pieces, maximizing sawmill wood

volume. The lower-performing plantations, such as P-1 and P-2, were optimized for smaller pieces, resulting in a more limited use of the material.

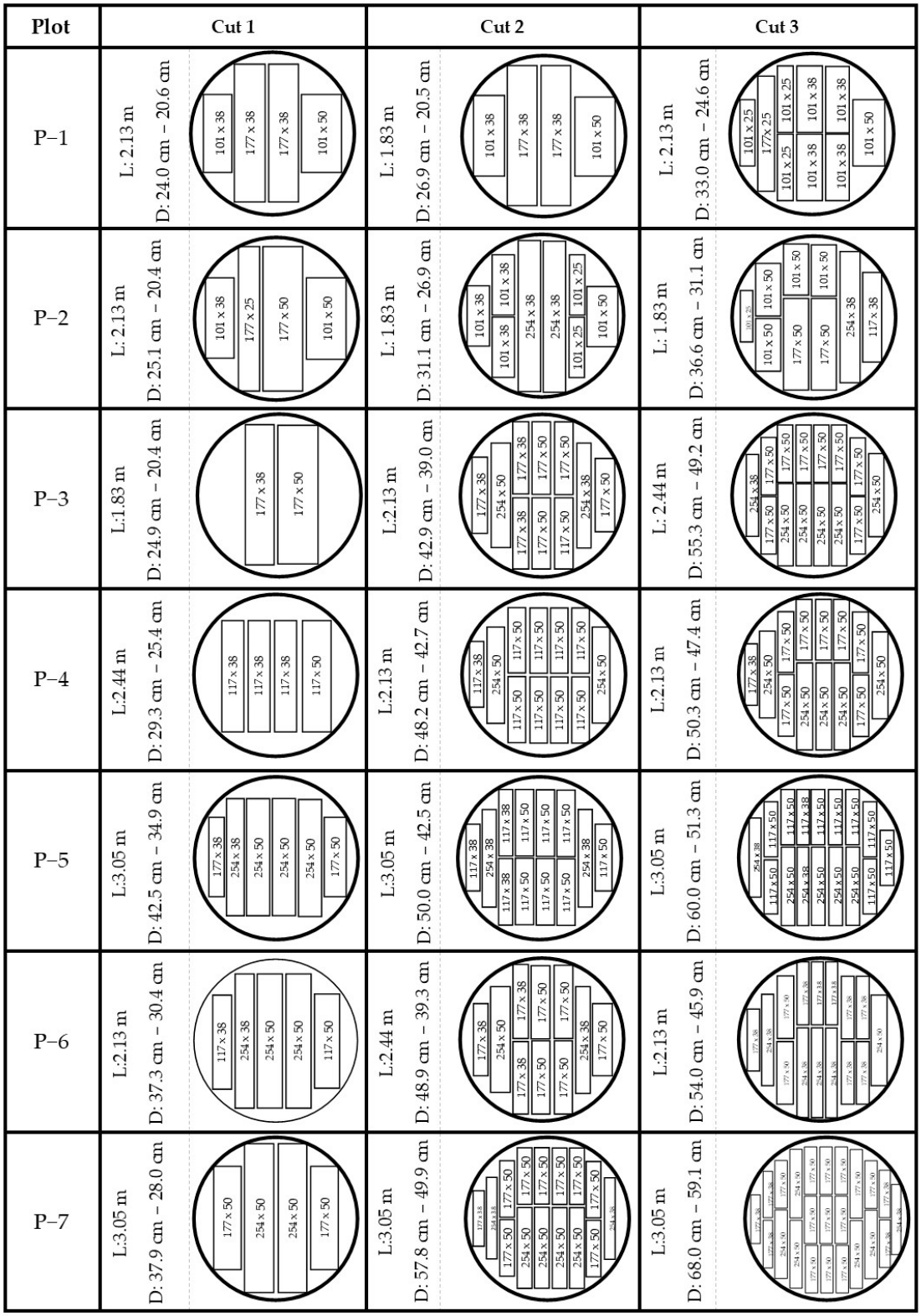

Figure 9. Wood-cutting optimization to maximize yield in different plantations for *Cedrelinga cateniformis* in the Peruvian Amazon. L denotes the length of logs, and D represents log diameters. The dimensions of the pieces are shown in mm.

4. Discussion

4.1. Analysis of the Diameter Structure and Diameter–Height Relationship

The results obtained in this study reveal how age and plantation type influence the diameter distribution of *Cedrelinga cateniformis* trees. The young plantations (P-1 and P-2, both 10 years old) included large numbers of small-diameter trees distributed in few diameter classes, indicating that their populations are still at an early growth phase [60]. By contrast, the older plantations (P-5 and P-7) include trees in a wider range of diameter classes, as evidenced by P-5, which included 17 classes. This is consistent with the hypothesis that time establishment allows for greater maturation and the development of larger-diameter trees [61].

The type and spacing of planting significantly affected competition between trees. This was observed in plantations P-1 and P-2, which were of the same age but differed in the number of diameter classes and the number of individuals per class because they were established in different production systems (MF and SAF) and with different spacing (5 × 5 m and 15 × 5 m). The trees in MF have smaller diameters (7.5–27.7 cm), and those in the SAF have larger diameters (7.5–37.5 cm). The variations are generally attributed to combinations of factors such as site, genetic material, spacing, soil and climate [62]. Agroforestry systems yield benefits in terms of soil structure, fertility and pest control, which are reflected in greater growth of the higher diameter classes relative to established plantations [61]. Furthermore, [63] reported that agroforestry associations, particularly those involving Theobroma cacao and *C. cateniformis* in the Ecuadorian Amazon, increase soil fertility, carbon sequestration and overall productivity.

The diameter distribution also varied in plantations P-5 and P-6. Despite being close in age, the LF-type plantation exhibited faster growth in diameter classes due to lower tree density and less competition for plantation resources. This pattern is consistent with the findings of [64], who indicated that planting density significantly influences tree competition and growth patterns.

Analysis of height–diameter (*dbh-H*) curves for *C. cateniformis* across seven plantations (P-1 to P-7) revealed significant variations influenced by factors such as planting distance, plantation age and species associations. Younger plantations (P-1 and P-2, 10 years old) exhibited more dynamic height growth with lower diameter accumulation, resulting in a better model fit. In mature plantations (P-5, P-6 and P-7), growth stabilized due to age-related limitations in resources. Planting distances of between 5 × 5 m and 10 × 10 m (as in P-1, P-5 and P-6) may favor a balance between height and diameter by effectively regulating competition. Plantation P-4 (12 × 8 m, "five-petal" design) has more balanced spacing, but the dispersion of resources among associated species and its age (25 years) seem to generate higher variability in data, reflected in the low R^2 of 0.14. Plantation P-6 combines moderate lateral competition and lower density, favoring relatively uniform growth, although the model fit is poorer than that for other mature plantations (R^2 = 0.61), probably due to variability in associated species and soil conditions. A good fit (R^2 = 0.69) was obtained for the plantation (P-7) with the densest spacing (2.7 × 2.7 m), probably due to intensive competition regulating uniform growth in both height and diameter. Simple associations, as in P-1 and P-5 (*C. cateniformis* + *Centrocema macrocarpum*), promote more homogeneous growth by reducing interspecific competition. Complex associations, as in P-4 (*Bertholletia excelsa* and *Theobroma grandiflorum*), create greater heterogeneity in resource competition, probably explaining the high data dispersion and low coefficient of determination.

Statistical modeling of tree growth often reveals significant variability based on environmental factors and species interactions. The low coefficient of determination values indicating data variability in certain plantations is consistent with the findings of broader

research highlighting how ecological complexity and soil conditions can influence model accuracy and the predictability of growth patterns [45,65].

4.2. Evaluation of Taper Models

Taper models are mathematical tools that describe stem diameter variation along the height of a tree, essential for estimating wood volume in different tree sections [66]. These models enhance forest resource planning by aiding commercial and residual volume estimation, thus maximizing production efficiency [67]. Additionally, taper models support forest management by enabling simulations that optimize wood yield under varying silvicultural practices and environmental conditions, and they provide reliable growth projections for sustainable forest management programs [68]. They provide estimates of diameter, total volume and individual log volumes, which are crucial for informed decision-making in these areas [69].

Various statistical models are used to describe taper. These include single models, segmented models, polynomial models and sigmoid models [60]. In our study, tree form was observed to vary across different plantations, as indicated by differing parameter values among plantations within the same model. This variation highlighted the need to identify the most suitable model to ensure greater accuracy. The Cielito II model demonstrated a trend closely aligned with observed data from the base, indicating an initially relatively consistent relationship between d/dbh and h/H across all plantations; however, deviations were observed in the upper sections. This may be due to greater variability in the height–diameter relationship at the top of the tree, which these models do not capture fully. A comparable pattern was observed in the Cervera model, wherein the superior aspects of the curves exhibited a tendency to widen in an outward direction. By contrast, the Garay model produced consistent curves across all plantations, with data points closely aligning with the model curves, suggesting a more stable relationship between d/dbh and h/H.

The Cielito II model (for plantation P-1) and the Cervera model (for plantation P-4) yielded high adjusted R^2 values and low RMSE; likewise, the Garay model yielded the highest adjusted R^2 in the other five plantations while maintaining low RMSE and Bias% values, indicating a minimum prediction error. The results of the analysis highlight the importance of not only the statistical indicators but also biological realism, where the Garay model best represented the stem profile of the species. These results are consistent with those of [70], who also found that the Garay model is optimal for estimating stem narrowing in eucalyptus clones (*Eucalyptus grandis* × *Eucalyptus urophylla*) in three agrosilvopastoral systems. Likewise, in some reports the Garay model was successfully applied to other species distributed in monoculture forest plantations, including the eucalyptus clone (*Eucalyptus grandis* × *Eucalyptus urophylla*) [71], pine (*Pinus taeda*) [72], teak (*Tectona grandis*) [73], and species distributed in native forests, including the baboon (*Virola surinamensis*) [74]. This demonstrates the adaptability of the model to different forest environments.

The good performance of the Garay model in various contexts can be attributed to its sigmoid structure, which is well suited to capture non-linear growth patterns typical of biological systems [60]. This structure may allow the model to reflect the different tapering tendencies of the *Cedrelinga cateniformis* stem in different production systems due to its ability to reflect the gradual narrowing of the stem from the base to the top.

On the other hand, studies in agroforestry systems have found that other models are effective under certain conditions. For example, [75] identified the Kozak model as providing the most accurate estimates of tapering for African mahogany (*Khaya ivorensis*), with RMSE values below 2.62% at different sites. The Kozak model was also reported to be the best-performing model selected in teak plantations, exhibiting an exceptional fit, with

an R^2 of 0.979 and a residual standard error (RSE) of 0.7868 [76]. Similarly, [77] identified the Biging model as optimal for *Pinus arizonica* in southwestern Chihuahua, emphasizing its compatibility with volume equations and utility in forest inventories.

Correct selection of the trunk profile model is essential. It has been shown that when using mathematical programming for multi-product optimization, the Ormerod and Kozak functions were essential for quantifying sections of length and diameter of tree trunks and that the exponential model outperformed the polynomial model by achieving a 16% increase in the use of material [78]. Therefore, stem profiling studies are needed to determine the model that is biologically most realistic for the management and optimization of forest products.

Application of the Garay model to all plantations not only facilitates analysis but also provides a foundation for sustainable management practices based on the ecological behavior of the species by small and medium forest producers due to the simplicity of use of the model compared with segmented models. The application of the selected model will improve volume estimates, optimize the harvesting process to reduce waste and maximize the utility of each tree. This precision increases the profitability of harvested wood and promotes sustainable management by ensuring that only the amount of wood required is harvested.

4.3. Model Optimization for Log and Saw Lumber Cutting in Cedrelinga cateniformis

4.3.1. Production and Log Cutting Optimization

Forest plantations are increasingly recognized to be essential sources of wood products, providing materials for a wide variety of uses while simultaneously reducing pressure on natural forests [5,79]. Products from these plantations include logs, sawn timber, wood pulp and other processed wood products.

The study findings showed that log dimensions vary between plantations. Short logs (1.83–2.13 m) were predominantly found in plantations P-1, P-2 and P-3 due to smaller tree diameters and shorter usable log lengths. Medium-length logs (2.44–2.74 m) appeared in plantations with more mature trees, such as P-3, P-4 and P-6. These lengths indicate a progression in tree maturity, although they are influenced by spatial constraints and competition between species. Long trunks (3.05 m) are more abundant in plantations P-5 and P-7 and are associated with the different plantation systems and advanced ages of 29 and 35 years, respectively. These longer trunks, linked to larger diameters, offer commercial advantages, maximizing trunk quality for applications requiring long and uniform pieces.

In general, trees with larger diameters tend to produce longer trunks, as the length of the trunk that is useful for the tree's purposes increases with diameter. This phenomenon was particularly evident in plantations P-5 and P-7, where the longest trunks reach up to 3.05 m in length. This outcome is linked to the maturation of the trees within these systems. In plantations with a larger diameter and lower-density trees, it is possible to harvest longer trunks, which is advantageous for high-value uses in the wood market. By contrast, plantations with smaller diameters, such as P-1 and P-2, result in shorter trunks, with lengths of 1.83 and 2.13 m, respectively. This indicates that in younger forest systems, trunk length is constrained by the smaller dimensions of tree trunks.

Although plantations P-1 and P-2 are both 10 years old, they yielded slightly different log volumes: 29.80 m^3ha^{-1} in P-1 and 26.86 m^3ha^{-1} in P-2. The higher volume in P-1 can be attributed to its configuration as a forest massif (FM) system, which promotes linear growth and competition between trees of the same species. This results in higher tree volumes at early ages. By contrast, P-2, an agroforestry system (AFS), yielded lower volumes due to competition with other fruit and forest species in the system.

Plantations P-5 and P-6 are close in age, at 29 and 28 years, respectively, but P-5 yielded a significantly higher total volume of 184.75 m^3ha^{-1} compared with 88.66 m^3ha^{-1} in P-6. This difference is due to tree spacing, with the linear configuration of P-5 enabling higher diameter growth due to minimal lateral competition, resulting in trunks up to 3.05 m long. This shows that while density is lower, larger diameters support higher volumes in long trunks, a highly valued feature in the wood market.

Volume analysis based on trunk length and diameter highlights the critical role of plantation systems and tree structure in *C. cateniformis* wood production. Forest agroforestry and live fence systems produce high volumes and long trunks at early and advanced stages, respectively. Agroforestry systems balance wood production with the timber volumes of other forest species and biodiversity. This analysis supports a differentiated management approach to optimize resources based on the structure and associations of each plantation. Furthermore, our results support [33,71], who emphasized the importance of logistic factors, wood type compatibility and choice of taper pattern, which significantly affect wood conversion to multi-product and subsequent income.

The distribution of log quantity and volume is the result of complex interactions between tree age, plantation type, plantation design and plantation spacing (Figure 7). These findings are consistent with existing reports, which show that forest management strategies that incorporate hierarchical optimization and consider stand structure and spacing result in higher volumes at the tree level [80]; similarly, zonation and spatial optimization approaches can maximize wood production targets [41].

4.3.2. Production and Sawn Lumber Cutting Optimization

The different types of plantations studied influenced the volumes and dimensions of sawn timber. The forest massif (P-1) slightly surpassed the agroforestry system (P-2) of similar age in terms of productivity. This may be due to the structure of each plantation, as the massif included a greater number of trees per hectare, but the SAF is characterized by trees with larger diameters and thus higher sawing yield (57.3% compared with the 51.2% for the MF). The P-1 plantation was characterized by generating short and thin pieces of wood, being able to saw five dimensions of up to 17.78–3.81 cm wide and thick; the opposite applied to plantation P-2, which yielded up to eight dimensions of up to 25.40–3.81 cm wide and thick were obtained.

Agroforestry systems, as in plantations P-3 and P-4, are characterized by a diverse production of pieces of wood of variable dimensions and lengths. This diversity is due to differences in species and spacing, enabling the production of both small and large pieces. The range of lengths, from 1.83 m to 3.05 m, makes these systems versatile, providing wood suitable for uses ranging from lightweight formwork to robust structural applications. Plantation P-4, for example, of age 25 years, produced a significant volume of medium-length pieces (up to 2.44 m), with thicknesses ranging from 3.81 to 5.08 cm. This variety benefits agroforestry systems by optimizing land use and providing a wide range of wood products.

Plantations P-5 and P-6 have contiguous ages, but the living fence or boundary system is notable for producing long and voluminous pieces at 29 years. While the width and thickness of these pieces remain standardized (17.78 to 25.40 cm wide and 3.81 to 5.08 cm thick), their lengths reach up to 3.05 m. The linear plantation configuration of this system minimizes lateral competition, encouraging vertical growth and resulting in longer pieces of wood. Such attributes make this wood ideal for high-demand structural or construction lumber applications.

Plantation P-7, of age 35 years, yielded a total wood volume of 333.60 m^3ha^{-1}, and it was particularly notable for its ability to produce pieces up to 3.05 m long. The longer

pieces of wood significantly improve the total usable volume and are particularly valuable for structural applications and high-value commercial products.

Detailed analysis of the sawn wood, based on the length and dimensions of the logs, revealed significant differences in productivity between the various plantation systems. The forest massif was distinguished by the production of short, thin wood. The agroforestry systems generated a range of products, encompassing small, thin pieces, as well as medium and robust pieces. This flexibility allows for the adaptation to diverse market demands while promoting ecosystem health and long-term sustainability. The living fence system focuses on producing longer and more voluminous pieces, optimizing the vertical growth of trees; this system is particularly advantageous for applications requiring wood with significant dimensions. The findings highlight the importance of aligning the choice of plantation system with production objectives, considering the desired wood products and sustainability goals.

In plantations P-1 and P-2, smaller log ends limit the production of larger pieces, leading to greater waste of material. By contrast, the most productive plantations, such as P-4, P-5 and especially P-7, have larger trunk ends (up to 25.40 cm), enabling cuts that maximize the volume of large pieces. The greater trunk diameter and length in these plantations allow for denser cutting configurations, reducing waste and improving wood utility. These findings are consistent with others reported for the species [81], where higher yields were obtained in trees belonging to the higher diameter classes. It is essential to ensure the timely implementation of forest management measures to optimize resource utilization, pruning and thinning [82,83]. The distribution of volume and number of sawn lumber pieces of *C. cateniformis* across various plantations is influenced by factors such as tree age, plantation type and planting spacing, which in turn affect the size and shape of the logs produced (Figure 8).

Our findings, together with those of [84], demonstrate the potential for improving volumetric yield and, thus, the competitiveness of small- and medium-sized sawmills through advanced decision support systems. Other authors [85] have also highlighted that the implementation of dynamic programming algorithms in cutting patterns improves raw material yields by 14%, demonstrating the practical benefits of integrating such technologies into sawmill operations. It is also important to consider that *C. cateniformis* plantations should be harvested before 30 years of age in order to maximize usable wood volumes [45]. Optimization studies produce satisfactory results, but they must also be validated in the field to verify their effectiveness [86], so it is recommended to use the dimensions of the logs and sawn pieces of wood from this field study as a guide.

According to reported statistics, Amazonian forests produce an average timber volume of 7.5 m^3ha^{-1} [87]. In the present study, the volumes of standing wood, logs, and sawn wood were much higher; therefore, the results of the research demonstrate that forest plantations are sustainable alternatives for wood production in degraded areas of the Peruvian Amazon. This finding highlights the need to formulate policies that facilitate the establishment of wood plantations, particularly in light of the fact that harvesting wood from natural forests is increasingly occurring in more distant locations and that issuing permits for such harvesting is constrained by administrative and legislative considerations [88].

5. Conclusions

The stem shape of *Cedrelinga catoniformis* varied among the plantation types studied. The Garay model performed best for modeling stem profiles, yielding high predictive accuracy and biological realism, with adjusted R^2 values up to 0.963.

Plantation design, combined with tree age, significantly influenced timber yields, with agroforestry systems providing various product dimensions and living fences producing

the longest and largest pieces, with log and sawn lumber volumes of up to 508.1 and 333.6 m^3ha^{-1}, respectively.

Dynamic programming of optimization techniques showed significant potential for maximizing the volume and yields of wood products and reducing waste.

Optimization techniques using dynamic programming showed significant potential for maximizing the volumetric yields of wood products and reducing waste.

The proposed approach provides a replicable model for optimizing forest resources, contributing to forest management in the Peruvian Amazon.

Future research should explore alternative stem profile models for other native species to enhance the optimization framework, and a cost–benefit analysis should be conducted to evaluate the economic feasibility of these techniques in various plantations.

Supplementary Materials: The following supporting information can be downloaded at https://www.mdpi.com/article/10.3390/f16010164/s1.

Author Contributions: Conceptualization, J.R.B.-V., G.G.C., G.Q.-B., C.A.A.J., P.Á.-Á. and H.G.L.; methodology, J.R.B.-V., G.G.C., G.Q.-B., C.A.A.J., P.Á.-Á. and H.G.L.; software, J.R.B.-V., G.G.C. and C.A.A.J.; validation, J.R.B.-V., G.G.C., G.Q.-B., C.A.A.J., T.S.C.T., Y.L.R.-P., G.V.-T., P.Á.-Á. and H.G.L.; formal analysis, J.R.B.-V., G.G.C., A.F.-S., E.J.S.-H., G.P.C.-R., T.S.C.T., Y.L.R.-P. and G.V.-T.; investigation, J.R.B.-V., G.G.C., R.P. and P.Á.-Á.; resources, J.R.B.-V., A.F.-S., E.S, G.P.C.-R., R.P., T.S.C.T., Y.L.R.-P., G.V.-T. and P.Á.-Á.; data curation, J.R.B.-V., G.G.C., G.Q.-B., C.A.A.J., P.Á.-Á. and H.G.L.; writing—original draft preparation, J.R.B.-V., G.G.C., A.F.-S., G.V.-T.; writing—review and editing, A.F.-S., E.J.S.-H., G.P.C.-R., T.S.C.T., Y.L.R.-P., G.V.-T., G.Q.-B., C.A.A.J., P.Á.-Á. and H.G.L.; visualization J.R.B.-V., G.G.C., R.P. and P.Á.-Á.; supervision, A.F.-S. and E.J.S.-H.; project administration, J.R.B.-V. and A.F.-S.; funding acquisition, J.R.B.-V., A.F.-S. and E.J.S.-H. All authors have read and agreed to the published version of the manuscript.

Funding: This research was financed by the National Forestry Program of the National Institute for Agrarian Innovation and the "Programa Presupuestal 121—Mejora de la articulación de los pequeños productores a los mercados".

Data Availability Statement: The data presented in this study are available on request from the corresponding author. The software is free and can be requested directly from the corresponding or last author (jrbasellyv@gmail.com and hgleite@ufv.br).

Acknowledgments: The authors thank the technical team of the National Forestry Program of the San Roque Experimental Station for the support provided (Edwin Leil Pinedo Tello, Max Machoa Java and José Luis Teagua Paima). Likewise, they thank the company INDUSTRIA MADERERA SAN JUAN S.AC.

Conflicts of Interest: The authors declare no conflicts of interest.

References

1. Adhikari, S.; Ozarska, B. Minimizing Environmental Impacts of Timber Products through the Production Process "From Sawmill to Final Products". *Environ. Syst. Res.* **2018**, *7*, 6. [CrossRef]
2. FAO. *El Estado de Los Bosques Del Mundo 2024*; FAO: Rome, Italy, 2024; ISBN 978-92-5-138875-4.
3. FAO. *Global Forest Resources Assessment 2020*; FAO: Rome, Italy, 2020; ISBN 978-92-5-132581-0.
4. Edberg, S.; Tigabu, M.; Odén, P.C. Commercial Eucalyptus Plantations with Taungya System: Analysis of Tree Root Biomass. *Forests* **2022**, *13*, 1395. [CrossRef]
5. Ratnasingam, J.; Ioras, F.; Farrokhpayam, S.R.; Mariapan, M.; Latib, H.A.; Liew, K.C. Perceptions by Smallholder Farmers of Forest Plantations in Malaysia. *Forests* **2021**, *12*, 1378. [CrossRef]
6. Carte, L.; Hofflinger, Á.; Polk, M.H. Expanding Exotic Forest Plantations and Declining Rural Populations in La Araucanía, Chile. *Land* **2021**, *10*, 283. [CrossRef]
7. Afonso, R.; Miller, D.C. Forest Plantations and Local Economic Development: Evidence from Minas Gerais, Brazil. *Policy Econ* **2021**, *133*, 102618. [CrossRef]

8. Viani, R.A.G.; Vidas, N.B.; Pardi, M.M.; Castro, D.C.V.; Gusson, E.; Brancalion, P.H.S. Animal-Dispersed Pioneer Trees Enhance the Early Regeneration in Atlantic Forest Restoration Plantations. *Nat. Conserv.* **2015**, *13*, 41–46. [CrossRef]
9. Barlow, J.; Mestre, L.A.M.; Gardner, T.A.; Peres, C.A. The Value of Primary, Secondary and Plantation Forests for Amazonian Birds. *Biol. Conserv.* **2007**, *136*, 212–231. [CrossRef]
10. Stimm, B.; Beck, E.; Günter, S.; Aguirre, N.; Cueva, E.; Mosandl, R.; Weber, M. Reforestation of Abandoned Pastures: Seed Ecology of Native Species and Production of Indigenous Plant Material. In *Gradients in a Tropical Mountain Ecosystem of Ecuador. Ecological Studies*; Beck, E., Bendix, J., Kottke, I., Makeschin, F., Mosandl, R., Eds.; Springer: Berlin/Heidelberg, Germany, 2008; Volume 198, pp. 417–429. [CrossRef]
11. Kainyande, A.; Auch, E.F.; Okoni-Williams, A.D. The Socio-Economic Contributions of Large-Scale Plantation Forests: Perceptions of Adjacent Rural Communities in the Northern Province of Sierra Leone. *Trees For. People* **2022**, *10*, 100329. [CrossRef]
12. Prado, D. *Plantaciones Forestales, Más Allá de Los Árboles*; Colegio de Ingenieros Forestales de Chile AG: Santiago, Chile; CORMA: Concord, ON, Canada, 2016; ISBN 978-956-7660-02-5.
13. SERFOR. Registro Nacional de Plantaciones Forestales. Available online: https://sniffs.serfor.gob.pe/estadistica/es/tableros/registros-nacionales/plantaciones (accessed on 23 October 2024).
14. Guariguata, M.R.; Arce, J.; Ammour, T.; Capella, J.L. *Las Plantaciones Forestales En Perú: Reflexiones, Estatus Actual y Perspectivas a Futuro*; Center for International Forestry Research (CIFOR): Bogor, Indonesia, 2017; ISBN 9786023870530.
15. Flores Bendezú, Y. *Fichas Técnicas Para Plantaciones Con Especíes Nativas En Zona de Selva Baja*; Instituto Nacional de Innovación Agraria: La Molina, Perú, 2019.
16. SERFOR. Anuario Forestal y de Fauna Silvestre 2023. 2024. Available online: https://sniffs.serfor.gob.pe/estadistica/es/tableros/publicaciones/anuarios (accessed on 23 October 2024).
17. Angulo Ruíz, W.E.; Fasabi Pashanasi, H.; Ruíz Castro, G. *Crecimiento y Productividad de Plantación de Tornillo Cedrelinga Cateniformis Ducke, Establecida En La Amazonía Peruana*; Trabajo Presentado en el XII Congreso Nacional Forestal; CONAFOR: Lima, Perú, 2016.
18. Baluarte-Vásquez, J.R.; Alvarez-Gonzales, J.G. Modelamiento Del Crecimiento de Tornillo Cedrelinga Catenaeformis Ducke En Plantaciones En Jenaro Herrera, Departamento de Loreto, Perú. *Folia Amaz.* **2015**, *24*, 21. [CrossRef]
19. Baluarte Vásquez, J. El Control De Calidad De La Madera De Plantaciones, Una Alternativa Para Alentar El Cultivo De Árboles De Especies Forestales Maderables, Estudio De Caso De Cedrelinga Catenaeformis Tornillo. *Folia Amaz.* **2019**, *28*, 43–51. [CrossRef]
20. Haag, V.; Koch, G.; Melcher, E.; Welling, J. Characterization of the Wood Properties of Cedrelinga Cateniformis as Substitute for Timbers Used for Window Manufacturing and Outdoor Applications. *Maderas. Cienc. Y Tecnol.* **2020**, *22*, 23–26. [CrossRef]
21. Sears, R.R.; Cronkleton, P.; Polo Villanueva, F.; Miranda Ruiz, M.; Pérez-Ojeda del Arco, M. Farm-Forestry in the Peruvian Amazon and the Feasibility of Its Regulation through Forest Policy Reform. *For. Policy Econ.* **2018**, *87*, 49–58. [CrossRef]
22. Álvarez Gómez, L.; Ríos Torres, S. *Evaluación Económica de Plantaciones de Tornillo*; Cedrelinga Catenaeformis, En El Departamento de Loreto: Loreto, Peru, 2009.
23. Castellanos Niño, Y.; Marco, J. Optimización Del Aprovechamiento de Productos Maderables de Tres Especies Forestales Comerciales En El Departamento Del Guaviare (Departamento de La Amazonía Colombiana) (Optimization of the Use of Timber Products of Three Commercial Forest Species in the Department of Guaviare (Department of the Colombian Amazon)). *SSRN Electron. J.* **2023**. [CrossRef]
24. Insfrán Ortiz, A.; Rey Benayas, J.M.; Cayuela, L. Establishment and Natural Regeneration of Native Trees in Agroforestry Systems in the Paraguayan Atlantic Forest. *Forests* **2022**, *13*, 2045. [CrossRef]
25. Marquardt, K.; Milestad, R.; Porro, R. Farmers' Perspectives on Vital Soil-Related Ecosystem Services in Intensive Swidden Farming Systems in the Peruvian Amazon. *Hum. Ecol.* **2013**, *41*, 139–151. [CrossRef]
26. Putney, J.D.; Maguire, D.A. Response of Douglas-Fir Stem Profile to Operational Nitrogen Fertilization in Western Oregon. *For. Ecol. Manag.* **2021**, *496*, 119411. [CrossRef]
27. Adu-Bredu, S.; Bi, A.F.T.; Bouillet, J.-P.; Mé, M.K.; Kyei, S.Y.; Saint-André, L. An Explicit Stem Profile Model for Forked and Un-Forked Teak (*Tectona grandis*) Trees in West Africa. *For. Ecol. Manag.* **2008**, *255*, 2189–2203. [CrossRef]
28. Olofsson, K.; Holmgren, J. Single Tree Stem Profile Detection Using Terrestrial Laser Scanner Data, Flatness Saliency Features and Curvature Properties. *Forests* **2016**, *7*, 207. [CrossRef]
29. Tavares Júnior, I.d.S.; de Souza, J.R.M.; Lopes, L.S.d.S.; Fardin, L.P.; Casas, G.G.; Oliveira Neto, R.R.d.; Leite, R.V.; Leite, H.G. Machine Learning and Regression Models to Predict Multiple Tree Stem Volumes for Teak. *South. For. A J. For. Sci.* **2021**, *83*, 294–302. [CrossRef]
30. Giri, K.; Chandra, G.; Jayaraj, R.S.C.; Borah, R.K.; Kardong, P.; Borah, S.; Goswami, A.K. Regression Models for Estimating Stem Volume of *Aquilaria malaccensis* (Lam.) in North East India. *Environ. Chall.* **2021**, *5*, 100279. [CrossRef]
31. Sandoval, S.; Acuña, E. Stem Taper Estimation Using Artificial Neural Networks for Nothofagus Trees in Natural Forest. *Forests* **2022**, *13*, 2143. [CrossRef]
32. Otárola-Acevedo, E.; Linares-Bensimón, C. Tablas de Volumen Total y Comercial de Cedrelinga Catenaeformis Ducke "Tornillo" Para Plantaciones En Loreto, Perú. *Folia Amaz.* **2006**, *13*, 151. [CrossRef]

33. Campos, B.P.F.; Binoti, D.H.B.; da Silva, M.L.; Leite, H.G.; Binoti, M.L.M.; Binoti, M.L.M.d.S. Conversão de Árvores Em Multiprodutos Da Madeira Utilizando Programação Inteira. *Rev. Árvore* **2013**, *37*, 881–887. [CrossRef]
34. Soares, T.S.; do Vale, A.B.; Leite, H.G.; Machado, C.C. Otimização de Multiprodutos Em Povoamentos Florestais. *Rev. Árvore* **2003**, *27*, 811–820. [CrossRef]
35. Löwe, R.; Sedmíková, M.; Natov, P.; Jankovský, M.; Hejcmanová, P.; Dvořák, J. Differences in Timber Volume Estimates Using Various Algorithms Available in the Control and Information Systems of Harvesters. *Forests* **2019**, *10*, 388. [CrossRef]
36. Kaya, A.; Bettinger, P.; Boston, K.; Akbulut, R.; Ucar, Z.; Siry, J.; Merry, K.; Cieszewski, C. Optimisation in Forest Management. *Curr. For. Rep.* **2016**, *2*, 1–17. [CrossRef]
37. Binoti, D.H.B. *Computer Systems Applied to Forest Management*; Florestal, D.E.M., da Natureza, M.A.E.C., Utilização de, T.E., Eds.; Universidade Federal de Viçosa: Viçosa, Brazil, 2012.
38. Hoganson, H.M.; Meyer, N.G. Constrained Optimization for Addressing Forest-Wide Timber Production. *Curr. For. Rep.* **2015**, *1*, 33–43. [CrossRef]
39. Murray, A.T.; Church, R.L. Heuristic Solution Approaches to Operational Forest Planning Problems. *OR Spektrum* **1995**, *17*, 193–203. [CrossRef]
40. Qiu, H.; Zhang, H.; Lei, K.; Hu, X.; Yang, T.; Jiang, X. A New Tree-Level Multi-Objective Forest Harvest Model (MO-PSO): Integrating Neighborhood Indices and PSO Algorithm to Improve the Optimization Effect of Spatial Structure. *Forests* **2023**, *14*, 441. [CrossRef]
41. Serrano-Ramírez, E.; Valdez-Lazalde, J.R.; De los Santos-Posadas, H.M.; Mora-Gutíerrez, R.A.; Ángeles-Pérez, G. Optimización de La Producción Forestal Maderable y Conservación Del Ecosistema En Bosques Comunitarios En El Sur de México. *Bosque* **2019**, *40*, 195–204. [CrossRef]
42. Esquivel Quispe, D. Estimación de Carbono y Estructura Poblacional de Cedrelinga Cateniformis En El Santuario Nacional Megantoni, Cusco. *Cantua* **2024**, *21*, 14–19. [CrossRef]
43. Hausxwell, F.W.Z. Determinación Del Volumen Comercial de Ramas de "Cedrelinga Cateniformis" (Tornillo) en Función al Dap y el Área de Copa en un Bosque de Colinas, Región Ucayali. Bachelor's Thesis, Universidad Nacional de Ucayali, Pucallpa, Perú, 2023.
44. SENAMHI Mapa Climático Del Perú. Available online: https://www.senamhi.gob.pe/main.php?dp=loreto&p=mapa-climatico-del-peru (accessed on 23 October 2024).
45. Cardenas-Rengifo, G.P.; Baselly-Villanueva, J.R.; Chumbimune-Vivanco, S.Y.; Macedo-Ramírez, A.T.; Salazar, E.; Minaya, B.; Quintana, S.; Cabudivo, A.; Palma, S.S.A.; Álvarez-Álvarez, P.; et al. Using Acoustic Tomography to Model Wood Deterioration in Cedrelinga Cateniformis Ducke in the Peruvian Amazon. *Forests* **2024**, *15*, 778. [CrossRef]
46. Cruz, W.; Saldaña, C.; Ramos, H.; Baselly, R.; Cancán Loli, J.; Cuellar, E. Genetic Structure of Natural Populations of Cedrelinga Cateniformis "tornillo" from the Oriental Region of Peru. *Sci. Agropecu.* **2020**, *11*, 521–528. [CrossRef]
47. Team, R.C. *R: A Language and Environment for Statistical Computing*; R Foundation for Statistical Computing: Vienna, Austria, 2020.
48. Rentería, A.J.B.; Ramírez, M.H.; Zamudio, S.F. Sistema de Cubicación Para Pinus Cooperi Blanco Mediante Ecuaciones de Ahusamiento En San Dimas, Durango. In *Proceedings of the En CEVAG, El Sitio Permanente de Experimentación Forestal (SPEF) "Cielito Azul" a 40 años de su Establecimiento*; Instituto Nacional de Investigaciones Forestales, Agrícolas y Pecuarias: San Dimas, México, 2006; p. 135.
49. Clutter, J.L. Development of Taper Function from Variable Top Merchantable Volume Equations. *For. Sci.* **1980**, *26*, 117–120.
50. Amidon, E.L. A General Taper Functional Form to Predict Bole Volume for Five Mixed-Conifer Species in California. *For. Sci.* **1984**, *30*, 166–171.
51. Kozak, A.; Munro, D.D.; Smith, J.H.G. Taper Functions and Their Application in Forest Inventory. *For. Chron.* **1969**, *45*, 278–283. [CrossRef]
52. Demaerschalk, J.P. Converting Volume Equations to Compatible Taper Equations. *For. Sci.* **1972**, *18*, 241–245. [CrossRef]
53. Ormerod, D.W. A Simple Bole Model. *For. Chron.* **1973**, *49*, 136–138. [CrossRef]
54. Cervera, J.M. El Área Basimétrica Reducida, El Volumen Reducido y El Perfil. *Montes* **1973**, *174*, 415–418.
55. Garay, L. Tropical Forest Utilization System. In *VIII A Taper Model for the Entire Stem Profile*; Including Buttressing: Seattle, DC, USA, 1979.
56. COFORD. *IFER TreeModel—Irish Stem Profile & Single Tree Volume Equations*; COFORD: Co. Carlow, Ireland, 2013.
57. Finger, C.A.G. *Fundamentos de Biometria Florestal*; UFSM/ CEPEF/FATEC: Santa Maria, RS, USA, 1992.
58. Leite, H.G. *Conversão de Troncos Em Multiprodutos da Madeira Utilizando Programação Dinâmica*; Florestais, D.E.C., Ed.; Universidade Federal de Viçosa: Viçosa, Brazil, 1994.
59. Leite, H.G.; Campos, J.C.C.; Junior, G.G.d.P. Emprego de Um Modelo de Programação Dinâmica Para Conversão de Troncos Em Multiprodutos Da Madeira. *Rev. Árvore* **1995**, *19*, 447–465.
60. Campos, J.C.C.; Leite, H.G. *Forest Measurement: Questions and Answers*, 5th ed.; UFV: Viçosa, Brazil, 2017; ISBN 978-8572695794.

61. Fuentes, E.; Gómez, C.; Pizarro, D.; Alegre, J.; Castillo, M.; Vela, J.; Huaman, E.; Vásquez, H. A Review of Silvopastoral Systems in the Peruvian Amazon Region. *Trop. Grassl.-Forrajes Trop.* **2022**, *10*, 78–88. [CrossRef]
62. Hess, A.F.; Loiola, T.; Arruda de Souza, I.; Nascimento, B. Morfometría de La Copa de Araucaria Angustifolia En Sitios Naturales En El Sur de Brasil. *Bosque* **2016**, *37*, 603–611. [CrossRef]
63. Tinoco-Jaramillo, L.; Vargas-Tierras, Y.; Habibi, N.; Caicedo, C.; Chanaluisa, A.; Paredes-Arcos, F.; Viera, W.; Almeida, M.; Vásquez-Castillo, W. Agroforestry Systems of Cocoa (*Theobroma Cacao* L.) in the Ecuadorian Amazon. *Forests* **2024**, *15*, 195. [CrossRef]
64. Pizarro, D.; Vásquez, H.; Bernal, W.; Fuentes, E.; Alegre, J.; Castillo, M.S.; Gómez, C. Assessment of Silvopasture Systems in the Northern Peruvian Amazon. *Agrofor. Syst.* **2020**, *94*, 173–183. [CrossRef]
65. Murga-Orrillo, H.; Pashanasi Amasifuén, B.; Arévalo López, L.A.; Inuma, M.C.; Abanto-Rodríguez, C. *Cedrelinga catenaeformis* (Tornillo) in Natural and Agroforestry Systems: Dendrometry, Soil and Macrofauna. *Trees For. People* **2024**, *16*, 100577. [CrossRef]
66. Santiago-García, W.; Ángeles-Pérez, G.; Quiñonez-Barraza, G.; De los Santos-Posadas, H.M.; Rodríguez-Ortiz, G. Avances y Perspectivas En La Modelación Aplicada a La Planeación Forestal En México. *Madera Y Bosques* **2020**, *26*. [CrossRef]
67. Rodríguez-Toro, A.; Rubilar-Pons, R.; Muñoz-Sáez, F.E.; Cartes-Rodríguez, E.; Acuña-Carmona, E.; Cancino-Cancino, J. Modelo de Ahusamiento Por Tipo de Suelo Para Pinus Radiata En Las Regiones Del Biobío y La Araucanía, Chile. *Rev. Chapingo Ser. Cienc. For. Y Del Ambiente* **2016**, *22*, 203–220. [CrossRef]
68. Tamarit Urías, J.C.; De los Santos Posadas, H.M.; Aldrete, A.; Valdez Lazalde, J.R.; Ramírez Maldonado, H.; Guerra De la Cruz, V. Volume Estimation System for Individual *Tectona grandis* L. f. Trees through Compatible Taper/Volume Functions. *Rev. Mex. Cienc. For.* **2014**, *5*, 58–74.
69. Salekin, S.; Catalán, C.H.; Boczniewicz, D.; Phiri, D.; Morgenroth, J.; Meason, D.F.; Mason, E.G. Global Tree Taper Modelling: A Review of Applications, Methods, Functions, and Their Parameters. *Forests* **2021**, *12*, 913. [CrossRef]
70. de Aguiar Júnior, A.L.; de Oliveira Neto, S.N.; Müller, M.D.; Soares, C.P.B.; Pena, R.F.; Calsavara, L.H.F. Eucalypt Modeling as a Function of Spatial Arrangement in Agrosilvopastoral Systems. *Agrofor. Syst.* **2023**, *97*, 495–508. [CrossRef]
71. Campos, B.P.F.; Binoti, D.H.B.; Silva, M.D.; Leite, H.G.; Binoti, M.D.S. Effect of Taper Model Used on the Conversion of Trees in Boles into Multiproducts. *Sci. For.* **2014**, *42*, 513–520.
72. Nogueira, G.S.; Leite, H.G.; Reis, G.G.; Moreira, A.M. Influência Do Espaçamento Inicial Sobre a Forma Do Fuste de Árvores de *Pinus taeda* L. *Rev. Árvore* **2008**, *32*, 855–860. [CrossRef]
73. Leite, H.G.; Oliveira Neto, R.D.; Monte, M.A.; Fardin, L.; Alcantara, A.D.; Binoti, M.D.S.; Castro, R.V.O. Taper Models of Heartwood of *Tectona grandis* L.f. *Sci. For.* **2011**, *39*, 53–59.
74. Leite, H.G.; Gama, J.R.V.; da Cruz, J.P.; de Souza, A.L. Função de Afilamento Para *Virola surinamensis* (Roll.) Warb. *Rev. Árvore* **2006**, *30*, 99–106. [CrossRef]
75. Lopes, L.S.D.S.; Rode, R.; Pauletto, D.; Baloneque, D.D.; Silva, A.R.; Santos, K.N.F. Dos Ajuste de Modelos de Taper e Sortimento de Toras de Mogno Africano em Sistemas Agroflorestais em Belterra, Pará. *Rev. Agroecossistemas* **2018**, *10*, 18. [CrossRef]
76. Noda, I.; Himmapan, W.; Furuya, N.; Hitsuma, G. Taper Equations for Evaluating Private Plantation Teak (<<*Tectona grandis*>>) in Thailand. *Jpn. Agric. Res. Q. JARQ* **2023**, *57*, 329–343. [CrossRef]
77. Pompa García, M.; Javier Corral Rivas, J.; Antonio Díaz Vásquez, M.; Martínez Salvador, M. Función de Ahusamiento y Volumen Compatible Para Pinus Arizonica Engelm. En El Suroeste de Chihuahua. *Cienc. For. En México* **2009**, *34*, 117–134.
78. Díaz Palma, M. A Model of Optimization of Cutting Rules in Forestry Harvesting Considering Different Tapering Functions. Bachelor's Thesis, Universidad del Bío-Bío, Concepción, Chile, 2023.
79. Sedjo, R.A. From Foraging to Cropping: The Transition to Plantation Forestry, and Implications for Wood Supply and Demand. *Unasylva* **2001**, *204*, 24–32.
80. Sun, Y.; Jin, X.; Pukkala, T.; Li, F. Two-Level Optimization Approach to Tree-Level Forest Planning. *For. Ecosyst.* **2022**, *9*, 100001. [CrossRef]
81. Yepes-Alza, F.; linares-Bensimón, C. Rendimiento de Trozas Aserradas de Cedrelinga Cateniformis Ducke Obtenidas Del Raleo Silvicultural de Plantaciones en Jenaro Herrera, Loreto—Perú. *Folia Amaz.* **2007**, *16*, 115. [CrossRef]
82. Russo, D.; Marziliano, P.A.; Macrì, G.; Zimbalatti, G.; Tognetti, R.; Lombardi, F. Tree Growth and Wood Quality in Pure vs. Mixed-Species Stands of European Beech and Calabrian Pine in Mediterranean Mountain Forests. *Forests* **2019**, *11*, 6. [CrossRef]
83. Dong, L.; Lin, X.; Bettinger, P.; Liu, Z. How to Maximize the Joint Benefits of Timber Production and Carbon Sequestration for Rural Areas? A Case Study of Larch Plantations in Northeast China. *Carbon Balance Manag.* **2024**, *19*, 24. [CrossRef] [PubMed]
84. Ramos-Maldonado, M.; Muñoz, F.T.; Mora, P.; Venegas-Vásconez, D. Optimizing Cutting Log Operations in Softwood Sawmills: A Multi-Objective Approach Tailored for SMEs. *IEEE Access* **2024**, *12*, 128141–128150. [CrossRef]
85. Acevedo, C.; Ramos-Maldonado, M.; Aguilera, C.; Monsalve-Lozano, D. Optimización 3D de Patrones de Corte Para Trozas de Pino Radiata Con Cilindro Central Defectuoso. *Maderas. Cienc. Y Tecnol.* **2015**, *17*, 2. [CrossRef]
86. Zamora, I.A.; Sanz, M.C.; Fernández, V.P. Modelo de Estimación de Volumen de Madera Aserrada Que Emplea Variables de Árboles En Pie Para "Pinus Radiata" D. Don. *Cuad. La Soc. Española Cienc. For.* **2004**, 135–140.

87. FAO. *La Industria De La Madera En El Perú*; FAO: Rome, Italy, 2018.
88. López Pérez, J. Estado Actual Socio Económico y Tecnológico de La Industria Del Aserrío de Madera En La Provincia de Maynas—Loreto—Perú 2023. Bachelor's Thesis, Universidad Nacional de la Amazonía Peruana, Iquitos, Peru, 2024.

Disclaimer/Publisher's Note: The statements, opinions and data contained in all publications are solely those of the individual author(s) and contributor(s) and not of MDPI and/or the editor(s). MDPI and/or the editor(s) disclaim responsibility for any injury to people or property resulting from any ideas, methods, instructions or products referred to in the content.